Synthesis and Characterization of 58S Bioactive Glass Via CTAB Modified Sol Gel Method for In-vitro Biological Activities

Bethelhem Gashaw Ewnete

A Thesis Submitted to

The Department of Materials Science and Engineering

School of Mechanical, Chemical and Materials Engineering

Presented in Partial Fulfillment of the Requirement for the Degree of Master's in

Materials Science and Engineering

Office of Graduate studies

Adama Science and Technology University

June, 2024

Adama, Ethiopia

Synthesis and Characterization of 58S Bioactive Glass Via CTAB Modified Sol Gel Method for In-vitro Biological Activities

Bethelhem Gashaw Ewnete

Advisor: Fetene Fufa Bakare (PhD)

Co advisor: Tadele Hunde Wondimu (PhD)

A Thesis Submitted to

The Department of Materials Science and Engineering

School of Mechanical, Chemical and Materials Engineering

Presented in Partial Fulfillment of the Requirement for the Degree of Master's in

Materials Science and Engineering

Office of Graduate

Adama Science and Technology University

June, 2024

Adama, Ethiopia

Declaration

I hereby declare that this Master Thesis entitled "**Synthesis and characterization of 58S bioactive glass via CTAB modified sol gel method for in-vitro biological activities**" is my original work. That is, it has not been submitted for the award of any academic degree, diploma or certificate in any other university. All sources of materials that are used for this thesis have been duly acknowledged through citation.

_____	_____	_____
Name of student	Signature	Date

Recommendation

I/We the advisor(s) of this thesis, hereby certify that I/We have read the revised version of the thesis entitled "**Synthesis and characterization of 58S bioactive glass via CTAB modified sol gel method for in-vitro biological activities**" prepared under my/our guidance by Bethelhem Gashaw Ewnete submitted in partial fulfillment of the requirements for the degree of Master of Science in materials science and engineering. Therefore, I/We recommended the submission of revised version of the thesis to the department following the applicable procedures.

_____	_____	_____
Major Advisor	Signature	Date
_____	_____	_____
Co-advisor	Signature	Date

Approval

I/we, the advisor(s) of the thesis entitled "**Synthesis and characterization of 58S bioactive glass via CTAB modified sol gel method for in-vitro biological activities**" and developed by Bethelhem Gashaw Ewnete hereby certify that the recommendation and suggestions made by the board of examiners are appropriately incorporated into the final version of the thesis.

Major Advisor	Signature	Date
Co-advisor	Signature	Date

Approval of Board of Reviewers

We, the undersigned, members of the Board of Examiners of the thesis by Bethelhem Gashaw Ewnete have read and evaluated the thesis entitled "**Synthesis and characterization of 58S bioactive glass via CTAB modified sol gel method for in-vitro biological activities**" and examined the candidate during open defense. This is, therefore, to certify that the thesis is accepted for partial fulfillment of the requirement of the degree of Master of Science in Materials science and engineering.

Chairperson	Signature	Date
Internal Examiner	Signature	Date
External Examiner	Signature	Date

Finally, approval and acceptance of the thesis is contingent upon submission of its final copy to the Office of Postgraduate Studies (OPGS) through the Department Graduate Council (DGC) and School Graduate Committee (SGC).

Department Head	Signature	Date
School Dean	Signature	Date
Office of Postgraduate Studies, Dean	Signature	Date

ACKNOWLEDGEMENT

First I want to thank God for the strength and grace given to me during the difficult parts of finishing this task. I would like to express my gratitude to Adama Science and Technology University (ASTU) for providing me with the MSc opportunity and research funding to carry out this study. Foremost, I would like to express my deepest gratitude to my major advisor, Dr. Fetene Fufa for his continuous support, guidance and encouragement throughout my research and the write up of this thesis. The expertise, patience and insightful feedback have been invaluable in shaping my work. Throughout my academic research and daily life, his vast knowledge and wealth of experience have inspired me. I also want to extend sincere thanks to my co-advisor, Dr. Tadele Hunde, for his unwavering assistance and support. I would like to thank Tsion Chuni for her support throughout the research. For sample characterization, I would especially want to thank the National Taiwan university of science and Technology and Mr. Demeke Tesfaye for his assistance during sample characterization in ASTU. Thanks to Dr. Gebisa Bekele head of our department and all staff members of the Materials Science and Engineering department. My heartfelt appreciation goes to my family for their unwavering love, support and understanding. Last but not least, I would like to thank my classmates who have provided a stimulating and enjoyable environment in which to learn and grow.

TABLE OF CONTENTS

LIST OF TABLES

LIST OF FIGURS

LIST OF ACRONYMS

BG	Bioactive Glass
MBG	Mesoporous Bioactive Glass
BGN	Bioactive Glass Nanoparticles
HCA	Hydroxyl-Carbonate Apatite
HA	Hydroxyl Apatite
HAp	Hydroxyl Apatite
CTAB	Cetyltrimethyl Ammonium Bromide
FTIR	Fourier Transforms Infrared Spectroscopy
BET	Brunauer-Emmett-Teller
EDS	Energy Dispersive Spectroscopy
SBF	Simulated Body Fluid
MBG	Mesoporous Bioactive Glass
SEM	Scanning Electron Microscope
FESEM	Field-Emission Scanning Electron Microscope
TEM	Transmission Electron Microscope
SAED	Selected Area Electron Diffraction
TEOS	Tetraethyl Orthosilicate
TEP	Triethyl Phosphate
TGA	Thermogravimetric Analysis
DTA	Differential Thermal Analysis
XRD	X-Ray Diffraction
PEG	Polyethylene Glycon
DDA	Dodecyleamine

PVP	Polyvinyl Propylene
P123, F127	Triblock copolymers
PEO-PPO-PEO	Pluronics
PU	Poly Urethane
MTT	3-(4,5-dimethylthiazol-2-yl)-2,5-diphenyltetrazolium bromide) assay

ABSTRACT

The clinical methods for repairing bone defects caused by various reasons have significant drawbacks and limitations. Significant advances in the treatment of bone diseases were made possible by the discovery and development of bioactive glasses (BGs). They are uniquely able to stick to living tissues, including bone due to the development of hydroxyapatite (HAp) layer on its surface. These bioactive glasses (BGs) can be made using different types of catalysts and structure directing agents in order to synthesis bioactive glass with enhanced biological activities. The majority of utilized catalysts generate toxicity, rise or reduce the pH value and work at high concentrations. And many surfactants have limited surface areas, a poor capacity to create well defined mesoporous structure and a potential for toxicity, all of which may reduce the bioactivity, biocompatibility and biodegradability of the bioactive glass. Therefore, to address the issues, this study focuses on the evaluation of a bioactive glass synthesized by sol-gel process employing low concentration cetyltrimethylammonium bromide (*CTAB*) *as a structure directing agent and citric acid as a catalyst in which citric acid and CTAB work in concert to obtain the optimal CTAB concentration with a better characteristics of bioactive glass properties. Through adjusting CTAB concentration, stoichiometric samples of bioactive glass BG without CTAB (BG0), BG with 0.1 M of CTAB (BG1), BG with 0.3 M of CTAB (BG3) and BG with 0.5 M of CTAB (BG5) were synthesized. The samples were characterized using TGA, XRD, SEM, BET, TEM, SAED, EDS, and FTIR. Sample particles were soaked in simulated bodily fluid for in vitro bioactivity test and the creation of hydroxyapatite (HAp) layers on the soaked particles was analyzed using XRD, SEM and FTIR. The* 3-(4,5-dimethylthiazol-2-yl)-2,5-diphenyltetrazolium bromide) (*MTT) assay was used to test the in vitro biocompatibility and an in vitro biodegradability test was performed to measure the weight loss of the samples over time after soaking in simulated body fluid. According to the results, BG with 0.3M of CTAB (BG3) exhibited larger specific surface area with spherical shaped particles and pore volume with mesoporous structure as well as cell viability above 70% resulting in a better in vitro bioactivity, biocompatibility and biodegradability.*

Key words: Bioactive glass, Bioactivity, Biocompatibility, Biodegradability, Citric acid and CTAB.

CHAPTER ONE

1. INTRODUCTION

1.1Background

The materials that are currently commonly used to reconstruct or repair bone disorders have long been considered "biomaterials" due to their satisfactory performance over many years *(Cannio et al., 2021).* Medical therapies, treatment with medicines and occasionally surgical procedures are necessary in the case of bone degeneration, aging, trauma and other severe bone-related diseases such as osteoarthritis, osteoporosis, osteosarcoma as well as cancer and tissue loss from bone fractures *(Gao et al., 2024).* These procedures frequently involve the repair or reconstruction of skeletal components.

Mostly used materials were bioinert materials such as metals, ceramics and polymers. But rather than growing new tissues, they only serve to temporarily support the defects' structural integrity *(Gautam et al., 2022).* Autografts and allografts are mainstays of clinical practice today. In autografts, bone tissue is taken from patient's own body (from another site). These methods have a number of disadvantages, including donor site morbidity, pain and insufficient bone tissue, which is especially problematic in children and longer surgical procedures. Also, there is a chance of infection transfer when allograft tissue is taken from someone other than the person receiving the graft. Synthetic bone graft has been developed as viable solution to address these problems *(Shibuya & Jupiter, 2015).*

Scientists and researchers are constantly discovering ways to use the potential of bio-materials to enhance care and advance medical technology *(Ratner & Zhang, 2020).* The smooth integration of biomaterials, with living tissues offers advantages, including biocompatibility and reduced risks of rejection or adverse reaction *(Chen & Liu, 2016).* The necessity for body part reinforcement or replacement outside of transplantation sparked the creation of biocompatible materials with mechanical and functional capabilities. Researchers have the chance to customize and regulate the

properties of biomaterials, which offers a range of possibilities, for medicine and tissue engineering applications *(Dolan et al., 2019).*

The extraordinary qualities of bioactive glasses have revolutionized the field of biomaterials. These distinctive materials have created new opportunities for biomedical applications. One essential quality of bioactive glasses is their capacity to solidify bonds with biological tissues. Due to their biocompatibility, which ensures minimum adverse reactions when in touch with the human body, they are successfully incorporated into variety of medical devices and implant *(Mazzoni et al., 2021).* These glasses can enhance the integration of implants into bone tissue and exhibit excellent osteoconductivity and osteoinductivity properties, promoting bone growth and regeneration. Such developments in the field of implantology have contributed to better patient outcomes accelerated healing processes *(Shearer et al., 2023).* It is well knowledge that bioactive glass is biocompatible, biodegradable, and active substance *(Al-Harbi et al., 2021).* These characteristics are crucial for fostering bone repair *(Hu et al., 2020).* Bioactive glasses simulate bone regeneration by releasing osteogenic ions, forming hydroxyapatite and promoting surface reactivity *(Drevet et al., 2023).* These glasses form biologically active hydroxyl apatite layer, enhancing osteoblast adhesion and cell proliferation, leading to enhanced healing *(Leite & Mano, 2017; Zheng, Niu, et al., 2021).* Since the degree of interaction produced between the bioactive glass particles and body fluids is determined by the morphology of particles which in return determines the bioactivity and biodegradability of the bioactive glass, altering the composition, structure and surface features of bioactive glasses is now more feasible than to develop tailor made solutions that cater to patient requirements and facilitate healing *(Lee et al., 2009).* Therefore, amorphous and porous bioactive glasses are preferable to promote and stimulate differentiation of cells and tissues because of their high specific surface area, tunable porosity and controllable compositions *(Lei et al., 2020; Zheng, Sui, et al., 2021).* Due to their best morphology, microstructure, small size and, spherical particles which gives it good flow properties and its chemical structure being similar to that of hard tissues, mesoporous bioactive glasses (MBG) in which their pore dimensions are within the range of 2- 50nm has gained acceptance in bone repair and regeneration application *(Lei, Chen, Wang, & Zhao, 2009; Miao et al., 2013; Min et al., 2016).* Therefore, it is possible to synthesize BGs with improved specific surface area, pore volume, and pore size by employing a sol-gel technique in conjunction with various structure directing agents and catalysts (Deshmukh et al., 2020).

The capacity to synthesis using lower processing temperatures than traditional glass melting methods and produce materials with regulated composition, morphology and chemically pure material is one of sol-gel method's primary benefits *(Moghanian et al., 2017).* By carefully tailoring the synthesis parameters, such as precursor concentration and calcination temperature, the properties of these resulting bioactive glasses can be precisely controlled. Due to these the sol-gel synthesis process has advantages for producing bioactive glasses. This process allows bioactive glasses to exhibit enhanced surface reactivity and biodegradability, making them valuable in biomedical applications *(Saravanapavan et al., 2004).* Factors like pH level, synthesis temperature, catalyst source and addition of structural directing agents affect properties of BGs made using the sol-gel technique. The catalyst source plays a significant role on the hydrolysis reaction and shape of the sol practice *(Lei, Chen, Wang, Zhao, et al., 2009).*

Catalysts can improve the functioning and performance of bioactive glasses by stimulate particular reactions that improve the substance's bioactivity, biocompatibility and biodegradability. They are responsible for the breakdown of bioactive glass precursors and improve the gel structure to obtain controlled morphology and increase the ion exchange *(Bueno et al., 2021).* The induction of particular biological processes, such as cell adhesion, proliferation and the creation of mineral deposits that resemble bone, depends on this controlled ion exchange *(Lei et al., 2020).* Although base catalysts have been frequently used in sol-gel process to produce bioactive glass, there are several limitations to this approach. Reduced homogeneity, difficult reaction conditions, the addition of contaminants, difficulties in reaction kinetics control *(Baino et al., 2018; Brinker, 1988; Kaur et al., 2020).* Acidic catalysts encourage the hydrolysis of alkoxides. By reducing the pH and raising the portion concentration, they hasten the creation of silica networks, which leads to the deposition of more porous structure with larger surface area *(Bellucci et al., 2017; Rahaman et al., 2011).* And these enhances the release of ions in which it also improves the bioactivity and degradation behavior of bioactive glasses. In contrast to inorganic acids like nitric and hydrochloric acids, biological hydroxyl-carboxyl acids like acetic acid, malic acid, and citric acid have distinctive chemical structures that might affect the structure and morphology of materials made from sol-gels *(Kuo et al., 2021).* The sol-gel method uses stronger acids at high concentrations, like nitric acid or hydrochloric acid, in the inorganic acid catalyzed sol-gel processes *(Chakraborty et al., 2021).* At lower molar ratios, a number of different acids might act as catalysts and produce purer, concentrated, and bioactive BGs *(Vafa et al., 2021).* For instance,

the concentration of the acid solution needed to catalyze the hydrolysis of alkoxides can be significantly reduced by substituting citric acid for nitric acid *(Faure et al., 2015)***.** When the glass dissolves, inorganic acids can significantly lower the pH of the surrounding area. The biological systems' ability to maintain homeostasis may be disturbed by this abrupt pH drop, which could also harm or kill cells *(Islam et al., 2017; Thavornyutikarn et al., 2019).* This cytotoxicity can impair cell migration, growth, and proliferation, which lowers biocompatibility *(Kapoor et al., 2014; Thavornyutikarn et al., 2019)*. On the other hand, citric acid performs in low concentration, has few residuals that can be eliminated at low temperature and aids in adjusting the pH of the reaction mixture. This pH control is crucial because it has an impact on the surface morphology and reactivity of the glass particles, which in turn impacts how bioactive, biodegradable and biocompatible are bioactive glasses *(Lopes et al., 2019).*

The sol-gel method provides the opportunity to improve the characteristics of porous bioactive glasses. For porous glasses to be used in biomedical domains effectively, regulated synthesis is essential. The patterning of porosity in sol-gel-derived glasses is made possible by inclusion of structural directing agents in the synthesis process, which may have a major impacts on their bioactivity *(Aneb et al., 2023).* Porous biomaterials can be divided into three primary groups based on the distribution of pore diameters: microspores, mesoporous, and macrospores, which have pore sizes of 2 nm or less, 2-50 nm, and >50 nm, respectively. Third-generation bioactive glasses, or mesoporous bioactive glasses (MBGs), were developed in 2004 by combining supramolecular chemistry with the sol-gel method *(Yan et al., 2006; Yan et al., 2004).* Compared to non-mesoporous bioactive glass (NBG), MBG exhibits superior specific surface area and better pore volume which resulted in a better bioactivity and degradability *(Catauro et al., 2015; Hench & Jones, 2015; Wu & Chang, 2012).* Therefore, under suitable synthesis conditions, these surfactant molecules self-organize into micelles and are connected to the hydrolyzed silica precursors within the micellar interior by a hydrophilic tail (a hydrophobic section acting as a shield). By self-organizing, these micelles produce a structured mesophase. After surfactants are removed, a well-ordered mesoporous structure with a high surface area and porosity is produced *(Izquierdo-Barba et al., 2005).* The type and concentration of surfactants used, pH values, processing temperatures, and solvents are only few of the variables that may have an impact on the surfactants that direct the production of porous structure *(Zheng, Sui, et al., 2021).* Templates such as pluronics (PEO-PPO-PEO), Poly Urethane(PU), poly (ethyl glycol) (PEG) and Dodecyleamine (DDA) are

frequently utilized in the production of BGs. These surfactants, however produce toxic byproducts, which can affect the biocompatibility of the bioactive glass *(Peng et al., 2021; Wu & Chang, 2011).* Their individual particles are merged which results in poor defined individual crystallite boundaries such as PEG and P123*(Akrity Anand et al., 2019).* It has been demonstrated that cetyltrimethylammonium bromide (CTAB) surfactant form a mesoporous structure with defined individual crystallite boundaries *(Akrity Anand et al., 2019).* It allows for the controlled synthesis of bioactive glasses with specific properties, such as pore size and surface area *(Deshmukh et al., 2020; Migneco et al., 2020).* However, these surfactant is used at higher concentration resulting in aggregation and carbon contamination which lowers the bioactivity and biocompatibility of BGs (S.-J. Shih et al., 2016). In order to achieve effective bioactivity, biocompatibility and biodegradability, this paper employs citric acid as a catalyst and cetyltrimethylammonium bromide (CTAB) as a structure-directing agent at lower concentration to synthesis bioactive glasses and also examines the impact of the concentration of CTAB on in vitro bioactivity, in vitro biocompatibility, and in vitro biodegradability by varying the CTAB concentration.

1.2 Statement of problem

The most common standard for reconstructing bones with flaws is the use of metal, ceramics and polymer, which are made of bioinert materials that only provide a transient fix and do not cling to tissues or another method which is bone grafting that causes donor-site morbidity, poor anatomical match, disease transmission and additional surgery, therapies, time and cost *(Barone et al., 2011; Khalid et al., 2017; Nkenke & Neukam, 2014).* However, the discovery and creation of bioactive glasses resulted in substantial breakthroughs in the treatment of bone aliments. They possess a special capacity to adhere to living tissues, including bone. In synthesis process of bioactive glass compared to the conventional glass melting procedures which results in the formation of phase separation, inhomogeneity and irregularly shaped bioactive glass, the sol-gel process enables the production of highly homogeneous, better control over process parameters, chemically pure materials at lower processing temperatures and production of bioactive glasses with higher specific surface area and more amorphous and porous overall *(Vafa et al., 2021).* During the sol-gel technique adding structural directing agent provides a better bioactivity and biodegradability by forming porous structure. But most structural directing agent's individual particles are merged, have lower SSA, have poor well defined individual crystallite boundaries within the pores, show

crystalline phase and produce toxic byproducts *(Aklilu et al., 2023; A. Anand et al., 2019; Peng et al., 2021).* Therefore, CTAB surfactant that have high specific surface area, form a mesoporous structure with defined individual crystallite boundaries was used *(Akrity Anand et al., 2019; Deshmukh et al., 2020; Vichery & Nedelec, 2016).* Even though these surfactant is used to increase SSA, it is used at high concentration which results in more carbon contamination and lowers the bioactivity and biocompatibility of the glass (Akrity Anand et al., 2019; S.-J. Shih et al., 2016). But using CTAB surfactant at lower concentration results in a better bioactivity and biodegradable with biocompatible BGs. And mostly used catalysts with CTAB are bases, however, a sphere with well-defined mesoporosity will be lost as a result of its high pH value *(Chen et al., 2008; Xia & Chang, 2007).* It also result in less homogeneity and introduction of toxicity *(Kaur et al., 2020).* And inorganic acids are utilized in higher concentration, require stricter processing regulations, have lowest pH value and cause toxicity *(Kapoor et al., 2014; Thavornyutikarn et al., 2019)*. But organic acid catalyst, citric acid has the ability to control pH levels, can be performed at low concentration, have a few residuals that can be eliminated at low temperature, breaks down quickly and can be removed, easier to make a homogenous gel and cause no harmful or poisonous substances *(Andersson & Kangasniemi, 1991; Faure et al., 2015).*

The synthesis of BGs featuring effective biological activities has remained challenging. Hence forth, using CTAB as a structural directing agent at lower concentration and citric acid as a catalyst could possibly enable to make a spherical particle with a well-defined mesoporous structure and free from toxicity show a promising effect on the bioactivity, biocompatibility and biodegradability of the bioactive glass.

1.3 Objectives

1.3.1 General objectives

- To synthesis and characterize 58S bioactive glass via CTAB modified sol gel method for in-vitro bioactivity, biocompatibility and biodegradability.

1.3.2 Specific objectives

- To synthesis bioactive glass powder with sol gel method.
- To characterize thermal analysis, phase composition, surface morphology and elemental composition of the synthesized bioactive glass powders.
- To investigate the in vitro bioactivity and vitro biodegradability of synthesized bioactive glass powders using simulated body fluid (SBF).
- To examine in vitro biocompatibility of the bioactive glass powders using colorimetric assay (MTT).
- To investigate the CTAB concentration impact on in vitro bioactivity, biocompatibility and in vitro biodegradability of the synthesized bioactive glass powders.

1.4 Significance

This work is aimed at the synthesis of a mesoporous 58S bioactive glass by using lower concentration of CTAB and citric acid in the sol-gel synthesis process and evaluate the CTAB concentration impact on the bioactivity, biocompatibility and biodegradability of the bioactive glasses. The findings could lead to stronger bonds with tissues, accelerating healing in patients with bone defects or injuries. Biocompatibility is crucial in biomedical materials in which low concentration of CTAB assisted with citric acid proved to be biocompatible, regulating in better tolerated materials that minimize the risk of infections, allergies or inflammatory responses. And the combination of the CTAB and the citric acid in the sol-gel method offers advantages glass synthesis techniques, allowing precise control of properties like particle shape, homogeneity and porosity which is essential for creating a better bioactive and biodegradable bioactive glass. When it comes to the practical use of bioactive glasses, the new glass can be made more accessible and commercially viable by concentrating on optimizing the synthesis process using cost effective components. The research contributes to the advancement of healthcare technologies by

developing bioactive glass materials with a controlled bioactivity, biocompatibility and biodegradability.

1.5 Scope of the study

This research focuses on the synthesis of bioactive glass for evaluation of bioactivity, biocompatibility and biodegradability. During the synthesis of this bioactive glass, the sol-gel process is used in which the precursors were tetraethyl orthosilicate (TEOS, $Si(OC_2H_5)_4$), phosphoric acid (H_3PO_4), and calcium nitrate tetrahydrate ($Ca(NO_3)_2.4H_2O$). As a catalyst citric acid and as a structure directing agent CTAB were used. The synthesis process of 58S bioactive glass consists of 60% SiO_2, 36% CaO, and 4% P_2O_5. TGA, XRD, SEM, TEM, SAED, BET, EDS, and FTIR were used to characterize the synthesized bioactive glass. And soaking the produced samples in SBF solution for an in-vitro bioactivity test in which the production of apatite layers was also examined using, XRD, SEM and FTIR. MTT assay was used for in-vitro test to evaluate the cytotoxicity of the prepared sample at different concentrations and time point. Biodegradability was analyzed by immersing the glasses in the SBF.

CHAPTER TWO

2. LITERATURE REVIEW

2.1 Background

2.1.1 Bone disorder

Orthopedics faces a lot of difficulties because of bone deformities. Congenital or acquire factors, such as bone injuries brought on by outside pressures or the aftereffects of certain illnesses and operations, might contribute to their development *(Xue et al., 2022).* Large bone abnormalities are difficult to manage and there is still disagreement over the best approach to use *(Migliorini et al., 2021).* The goal of surgical care is to restore the lesion while preventing amputation and delivering satisfactory functional results *(Renard et al., 2000).* Large bone defect can be repaired using autografts, allografts and non-biological materials *(Nishida & Shimamura, 2008).* Given their characteristics of osteogenesis, osteoinduction, osteoconduction and histocompatibility, which result in a low risk of immunological rejection, autografts like vascularized iliac bone graft *(Arrington et al., 1996)* and vascularized fibular graft *(Ou et al., 2020)* are regarded as the best standard for reconstruction of post traumatic bone defects with non-union or mal-union *(Baldwin et al., 2019; Beaman et al., 2006).*

The limited supply of bone transplant, reoperation of the donor site, length wound drainage and infection are drawbacks *(Ghoneimy et al., 2019).* After removing a bone tumor, allograft are frequently employed as a viable substitute for autografts *(Delloye et al., 2007).* The relative abundance of these grafts , which enables repair even after a significant bone lesion and the lack of donor site morbidity are their key advantages *(G. N. Panagopoulos et al., 2017).* Conversely, the drawbacks include immunological rejection and the possibility of contracting contagious illnesses like HIV and Hepatitis C *(Mankin et al., 2005).* Segmental enndoprosthesis are the primary non-biological materials *(Zekry et al., 2019).* Segmental prosthesis have a number of benefits, including quick recovery, fast stability and early weight bearing *(Zheng et al., 2019).* On the other hand, the drawbacks include mechanical wear, periprosthetic fracture, prosthetic

infections and mechanical loosening *(Graci et al., 2010; Georgios N. Panagopoulos et al., 2017).* There is ongoing disagreement regarding the optimum surgical method and no agreement has been established.

The field of tissue engineering has recently made advancements that have given rise to a new bone repair treatment method. In order to regenerate bone tissue, bone tissue engineering uses scaffolds, cells and growth factors *(Xue et al., 2022).* The induced membrane technique (IMT), also known as the Masquelet technique, is a two-step surgical process that uses a temporary spacer to encourage the growth of a membrane surrounding the bone deficiency, which then removed and bone formation is encouraged *(Lu et al., 2021).* The use of 3D printing technology to treat critical sized bone lesions has showed potential. However, there is still a dearth of credible research that supports the usage of artificial bone substitutes *(Mayfield et al., 2022).* A strstegy for a systematic review is now being developed to look into the approaches for treating drill-hole abnormalities in animal model of bone healing *(Bromer et al., 2022).*

Recent work has showed encouraging outcomes for the treatment of bone defects using metals, polymers and ceramics. Ceramics are a time-honored biodegradable substance frequently used to mend bone defects *(Kim et al., 2020)*. However they can fracture under load and are therefore not suitable for use in load-bearing applications *(Amini et al.).* Ceramics may not be appropriate for use in major bone defects since they are not as robust as metals *(Xue et al., 2022).* Because of their exceptional mechanical characteristics, metals are perfect for bone restoration when it comes to load-bearing bone deformities *(Xue et al., 2022).* Non-degradable metals, however might result in long term issues such as corrosion, metal ion leakage and implant loosening. While biodegradable metals are a viable alternatives, their rate of degradation might not keep up with the rate of bone rebuilding, which could result in implant failure *(Zhang et al., 2021).* Due to their biodegradability, biocompatabiliity, ease of pproduction, superior mechanical qualities and minimal toxicity synthetic polymers have been employed for bone regeneration. They are unable to provide optimum bone growth when administered alone, though. Synthetic polymers might also provoke an inflammatory reaction and not be appropriate for use in load-bearing applications *(Zhang et al., 2021).*

Bioactive glass (BG), a type of glass created to interact with biological systems, has been employed in a number of fields, including orthopaedics, tissue engineering and dentistry. In addition to conventional surgery, a study from *(Cannio et al., 2021)*, indicated that bioactive glass was effective in treating intrabony deformities. It is a potential material for healing bone abnormalities because it has been demonstrated to exhibit osteoconductive, angiogenic and antibacterial characteristics. Mechanical strength is not a limiting factor in the use bioactive glass scaffolds for bone repair, according to an evaluate of bioactive glass scaffolds for bone tissue synthesis synthesis *(Fu et al., 2011).* Bioactive glass scaffolds are a promising method for repairing bone defects, according to a review of in-vivo experments using bone defect models. The use of bioactive glass scaffolds in promoting osseous regeneration was discovered to offer promising outcomes *(El-Rashidy et al., 2017).* An analysis of the utilization of bioactive glass for periodontal regeneration was published in 2023 after a thorough review. Bioactive glass proved helpful in reducing probing depth and raising clinical attachment level when compared to other materials *(Motta et al., 2023).* In a comprehenive review that investigate the use of bioactive glass for long bone infection published in 2016, it was discovered that the material was successsful in stimulating bone regeneration and lowering infection *(Aurégan & Bégué, 2015).*

2.1.2 Bioactive glasses

A class of biomaterials known as bioactive glasses has been researched for potential use in a range of biological applications. Amorphous silicate-based materials with the ability to create a potent chemical connection with tissues are known as bioactive glasses *(Hugo R. Fernandes et al., 2018).* The amorphous nature allows it to have a faster and controlled ion release mechanism, increased SSA and better dissolution rate due to its disorderd atomic structure *(Shearer et al., 2024).* The many forms of bioactive glasses include composites, porous scaffolds, bulk materials and powders *(Subramani & Ahmed, 2012).* The use of bioactive glasses in tissue engineering and regenerative medicine has recently attracted a lot of attention. They are advantageous in dentistry, reconstructive surgery and the management of infections due to certain qualities qualities *(Mahdi, 2019).* Additionally, some bioactive glasses has been enhanced with dopants like bismuth oxide to add antibacterial qualities for the treatment of bacterial bone infections *(Joy-anne et al., 2019).* Due to their great biocompatibilty, bioactive glass are an excellent choice for accelerating bone regrowth and wound healing. Bioactive glasses are appropriate for use in bone tissue engineering

and regeneration applications because they have a composition that is comparable to that of real bone *(Hugo R Fernandes et al., 2018).* They have calcium and phosphate contents that are comparable to bone hydroxyapatite, which makes them approptiate for fusing and integrating with bone tissues *(Jafari et al., 2022).* Since the bone is made up of crystal HAp, bone forming cells and collagen fiber, the idea behind the chemical composition of bioactive glasses is that the implant material should be able to generate the HAp layer on the surface in biological fluids *(Ingole et al., 2018)*. Glasses that have the potential to be bioactive can bind to tissues chemically and encourage the growth of hydroxyapatite on their surface *(Hugo R Fernandes et al., 2018).* It is simple to modify the composition of bioactive glasses, which gives the materials unique characteristics that can effectivey meet the needs of a wide range of biomedical applications *(Zhao et al., 2021).* Four BG classes exist, 1) 35-60wt% SiO_2, 10-50wt%CaO, and 5-40wt% Na_2O; bioactive and can adhere to soft tissues and bone, 2) <35wt% SiO_2; do not form glass, 3) >50wt% SiO_2, <10wt%CaO, <35wt% Na_2O; bone resorption in 10-30 days, 4) >65wt% SiO_2; not bioactive *(ÖZEL et al.).*

As shown by many researches the bioactivity of a bioactive glass can be affected by the crystallinazation of the bioactive glass which could be due to composition or synthesis method. These crystallinazation leads to a decrease in bioactivity of the bioactive glass which makes it bioinert material. On the other hand amorpous bioactive glasses exibit an increased bioactivity and degradability (Chen et al., 2006; Sepulveda et al., 2002).

The characteristics and applicabilities of bioactive glasses for bone therapy applications can be influenced by the synthesis process. The technique of choice must permit fine control of the glass composition and structure in order to be approprite for modifying particular qualities for bone therapy.

2.2 Synthesis methods

There are various techniques that can be used to create bioactive glasses, each with their own drawbacks. Melt-quench, spray pyrolysis, hydrothermal and sol-gel techniques are just a few of the ways bioactive glasses can be made. The precursor materials are heated to high temperatures during the melt-quench technique and then quickly cooled to create glass. This process is quite straightforward, although it may cause the production of undesirable crytalline phases and the loss

of volatile substances *(Cannio et al., 2021).* In the spray pyrolysis process, precursor materials are sprayed onto a hot substrate, where they are quickly dried and heated to produce glass. However, this is not preferred for the synthesis of bioactive glasses because to its limited control over particle size and morphology, development of undesirable phases, limited control over porosity and difficulty in managing the composition *(Hong et al., 2018; Shih et al., 2012; Workie et al., 2023).*

The production of bioactive glasses is frequently accomplished using the so called sol-gel method. In this process, metal alkoxides or metal salts are hydrolyzed and condensed in solution to create a sol, which is subsequently aged and dried to create a gel *(Deshmukh et al., 2020)*. After that, the resultant gel is heated to create a glass.

In comparison to conventional melt-quenching techniques, the sol-gel method has a number of benfits, such as improved composition control, product homogeneity and the potential to create glasses with a greater surface area and porosity. The application of bioactive glasses made from sol-gel has been studied in a number of biomedical disciplines, including dentistry, reconstructive surgery and the management of infection *(Cannio et al., 2021).* Due to their capacity to bind with bone tissue and encourage bone formation, these glasses have demonstrated potential for use as bone graft alternatives *(Deshmukh et al., 2020).* In instance, antimicrobial agents or growth factors have been added to mesoporous bioactive glasses made utilizing sol-gel techniques to produce therapeutic effects *(Cannio et al., 2021).*

The characteristics of bioactive glasses made from sol-gel have been the subject of numerous studies. The physical characteristics of melt-derived and sol-gel bioactive glasses were studied by Sepulveda et al., who discovered variations between the two processes *(Baino et al., 2018).* The regulated synthesis of these glasses is essential to their efficient usage in biomedical disciplines since the morphology and chemical makeup of porous bioactive glasses made from sol-gels greatly influence their biological capabilities *(Deshmukh et al., 2020).* It has also been possible to create bioactive glass nanoparticles (BGN) using the sol-gel process. The hydrolysis and condensation reactions have been started using various catalysts and the resultant BGN have been examined for their potential use in biomedical applications *(Zheng & Boccaccini, 2017).*

By modifying many parameters, including the hydrolysis rate, gelation time, aging, drying and calcination temperature, the sol-gel methode provides an easy and highly effective way for manufacturing porous bioactive glass *(Deshmukh et al., 2020).*

2.3 Bioactivity

A class of bioceramic materials known as bioactive glasses have numerous clinical uses. High biocompatibility, antibacterial properties, biodegradability and bioactivity in the internal environment of the body are only a few of their characteristics that have made them effective biomaterials in a variety of medical and dental sectors *(Jafari et al., 2022).* One of the most crucial characteristics of bioactive glasses is their bioactivity, which is defined as their capacity to establish a solid chemical interaction with tissues and encourage the production of hydroxyapatite on their surface *(Kaou et al., 2023).* The partial solubility of bioactive glasses in bodily fluids and the release of healing ions into the environment are the main causes of the production of this characteristics. Si ions, one of the primary constituents of bioactive glass, in particular, enhance angiogenesis, whereas Ca ions support osteogenic activity and cell growth *(Montazerian & Zanotto, 2017; Salinas et al., 2018).* The bonding layer between the bioactive ingredients and the live tissues is subsequently created by the HAp crystals. The in-vitro bioactivity of such bone bone-forming biomaterials is a crucial indicator of their in-vivo bioactivity since it describes how HAp behaves on biomaterials in a simulated body fluid (SBF). These HAp layer formation on the bioactive glasses can be examined using different characterizing technics after the immersion of the BGs in SBF. On XRD, HAp is indicated by the diffraction peaks that appeared after the immersion in SBF *(Chen et al., 2018).* These HAp formations can also be determined using FTIR which is indicated by the formation of P-O bond peak but sometimes these P-O bond could also indicate the presence of PO^{3-}_4 group in the glass structure, not apatite formation at around 1238cm^{-1} *(Letaïef et al., 2014). T*he morphology of the BG surface changes after immersion in SBF solution which is detected by SEM microscopy. These change is due to the formation of HAp indicated by the appetite grains, flower like or needle like clusters on the surface of BG particles *(Letaïef et al., 2014).* The development of the HAp layer may be complicatedly influenced by the chemical composition, chemical structure and textural characteristics (pore size, pore volume and pore structure) of biomaterials *(Arcos et al., 2002; Vallet-Regí et al., 1999).*

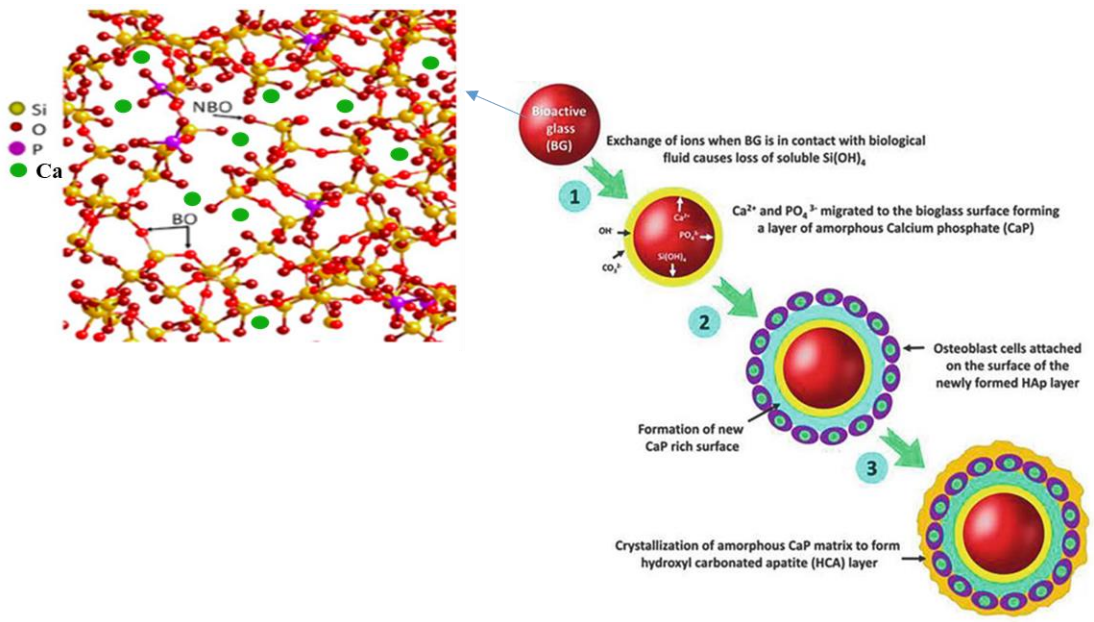

Figure 1. Illustration of series of ion exchanges involved in the formation of HA *(Joy-anne et al., 2019)*

The production of the apatite-like layer may be favored kinetically by increasing the pore size and pore volume of typical sol-gel derived BGs. Mesoporous bioactive glasses (MBGs), a new class of nanostructured glasses with improved textural and bioactive properties , have recently been created *(Vallet-Regí, 2010)*. Based on the distribution of pore diameters, porous biomaterials can be categorized into three main groups; microspores, mesoporous and macrospores, which have pore sizes of 2nm or less, 2-50nm and >50nm, respectively. MBGs are third-generation bioactive glasses that were created in 2004 using a mix of the sol-gel technique and surfactant supramolecular chemistry *(Yan et al., 2006; Yan et al., 2004).* In order to produce well-ordered mesoporous structures, surfactants including F127, P123, PEG and CTAB are typically utilized in the synthesis of MBG *(Salonen et al., 2005; Vallet-Regí et al., 2005).* These surfactant molecules self-organize into micelles under the right synthesis conditions and are linked to the hydrolyzed silica precursors inside the micellar interior by a hydrophilic tail (a hydrophobic section that serves as a shield). These micelles generate a structured mesophase by self-organization. A well-ordered mesoporous structure with a high surface area and porosity is obtained after the elimination of

surfactants *(Izquierdo-Barba et al., 2005)*. These $CaO\text{-}SiO_2\text{-}P_2O_5$ based compositions include mesoporous channels with highly organized pore diameters ranging from 2 to 50nm. MBG has superior in-vitro apatite formation ability in simulated body fluids (SBFs), excellent cytocompatibility and better pore volume when compared to non-mesoporous bioactive glass (NBG) *(Catauro et al., 2015; Hench & Jones, 2015; Wu & Chang, 2012)*. Mesoporous materials with a high degree of order are thought to be a very promising option for bone tissue engineering *(Baino et al., 2016; Hench & Polak, 2002)*. The in-vitro bioactivity of BGs is determined by the textural properties, which include specific surface area, pore volume pore size and pore shape. High in-vitro bioactivity of BGs can be induced by high specific surface area, high pore volume and narrow mesoporous size distribution *(Lei, Chen, Wang, & Zhao, 2009)*.

A study by *(Akrity Anand et al., 2019)* shows in Fig. 2 XRD pattern of different MBG powders calcined at 650ºC. MBG-CTAB powders as shown in Fig.2a exhibits a common diffusion halos at 20-35°2θ, that confirms amorphous nature of powders *(Letaief et al., 2014; Li et al., 2004)*. And as shown in Fig.2b MBG-PEG powder showed slightly crystalline phase of Ca_2SiO_4. MBG-P123 powder showed slight crystalline bi-phase and amorphocity as well in Fig.2c.

As Fig.3a shows in the field emission MBG-CTAB produces largely homogeneous, spherical particles when CTAB surfactants are used. For MBG-PEG and MBG-P123, spherical morphologies were also observed, however the individual particles are merged. The small particle size of the powders as they were created caused individual crystallites to fuse together, making it incredibly challenging to separate them. The use of the cationic surfactant CTAB resulted in the spherical morphology for MBG-CTAB. A study by *(Li et al., 2015)* shows that silica grows rapidly when TEOS is introduced, the arrangement of well-defined individual particulates is diminished when non-ionic surfactants such pluronic P123 and PEG are applied.

As given in Fig.3b, individual crystallite boundaries in MBG-PEG are poorly defined, but mesoporous are still clearly visible. In contrast, MBG-CTAB revealed individual crystallites in spherical shape with mesoporous structure inside. Although the mesoporous structure of the MBG-P123 particles was clearly delineated, individual crystallites were not visible.

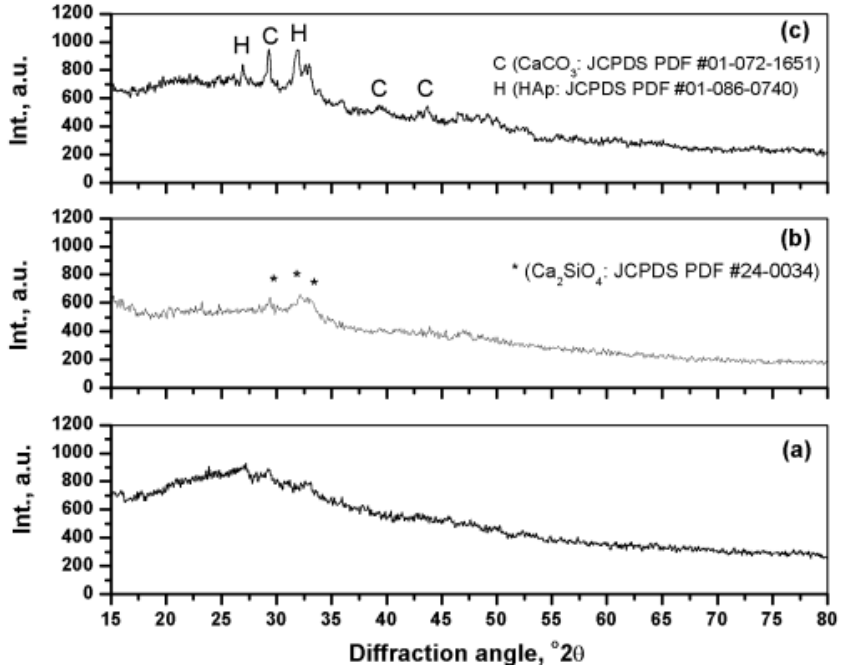

Figure 2. XRD pattern of MBG powders synthesized by different methods; (a) MBG-CTAB, (b) MBG-PEG and (c) MBG-P123 fired at 650°C *(Akrity Anand et al., 2019).*

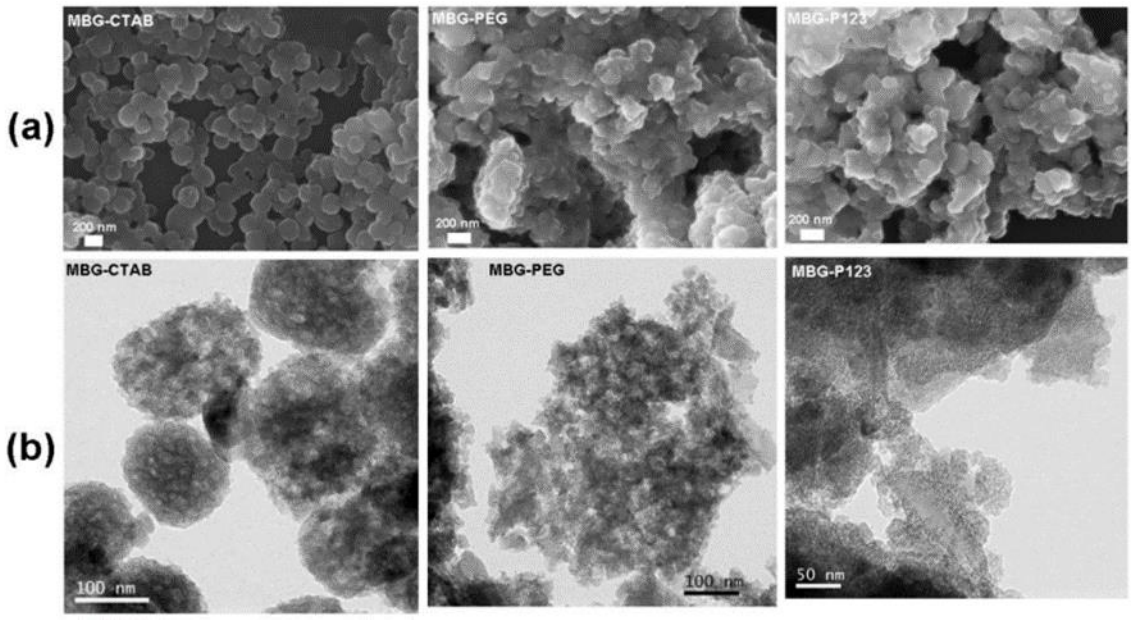

Figure 3. (a) FESEM powder morphology of different MBG powders; (b) TEM of the different MBG powders *(Akrity Anand et al., 2019).*

.

2.4 Biocompatibility

The appropriateness of bioactive glasses for usage in the human body is greatly influenced by their biocompatibility. Bioactive glasses have been demonstrated in in-vitro experiments to possess osteoinductive and osteoconductive properties, giving them a suitable option as grafts in periodontal regeneration *(Cannillo et al., 2022).* When implanted, bioactive glasses create a solid link with tissues, particularly bone *(De Caluwé et al., 2016).* Human bone marrow mesenchymal stem cells' ability to attach to, colonize and differentiate into osteoblasts on these biomaterials has demonstrated their capacity for regeneration *(Bellucci et al., 2020).* The use of cell culture for the assessment of new candidates as implant materials is one of the best methods to determine the biocompatibility of new materials; these studies provide useful information on the impact of the materials on the behavior of the cells. Cell viability above 70 % indicates the biocompatibility of the material *(Zheng et al., 2020).* The utilization of osteoblast cultures is of particular importance when examining the biocompatibility of bioactive glasses because the major clinical purpose for these materials is as a substitute for bone. In terms of promoting osteoblast differentiation and proliferation, bioactive glasses have been compared to non-reactive glasses and other biomaterials. Generally speaking, bioactive glasses enhance these biological processes better than other biomaterials *(Moghanian et al., 2021; Naruphontjirakul et al., 2022).*

The impact of the sol-gel technique on the biocompatibility of bioactive glasses for bone has been examined in a number of research. According to a study by *(Chen et al., 2006),* the sol-gel technique created bioactive glasses with a greater surface area and pore volume, increasing the material's bioactivity and biocompatibility. In a different study, *(Li & Chang, 2013)* demonstrated that the sol-gel process created bioactive glasses with a more homogenous structure, which enhanced the material's mechanical characteristics and biocompatibility. *(Vichery & Nedelec,* 2016) study created mesoporous bioactive glass utilizing the sol-gel process and it was discovered that the substance had good osteogenic and biocompatibility potential. MBGs are third-generation bioactive glasses that were created in 2004 using a mix of the sol-gel technique and surfactant supramolecular chemistry *(Yan et al., 2006; Yan et al., 2004).* To create well-ordered mesoporous structures, surfactants are typically utilized in the production of MBG. MBG has superior in-vitro apatite formation ability in simulated body fluids (SBFs), better pore volume and excellent

cytocompatability when compared to non-mesoporous bioactive glass *(Catauro et al., 2015; Hench & Jones, 2015; Wu & Chang, 2012).*

2.5 Biodegradability

A family of materials known as bioactive glasses has received extensive research due to its potential use in tissue engineering and regenerative medicine. These materials' biodegradability, or capacity to deteriorate over time when in touch with bodily fluids and be replaced by new bone formation and tissue regeneration, is a crucial feature. The degradation rate of sol-gel-produced bioactive glasses is crucial for bone grafting, as it affects cell attachment and growth, ultimately terminating the development of new bone. Biodegradable glasses, with their ionic dissolution products, promote vascularization, osteogenesis, and angiogenesis *(Solgi et al., 2017)*. However, controlling the degradation rate is challenging due to the complexity of the process. Bioactive glasses degrade in different ways depending on their composition, surface properties, shape, and environment.

The biocompatibility and rate of degradation of bioactive glasses are substantially influenced by their chemical makeup. When in contact with bodily fluids, bioactive glasses that include silica (SiO_2) create a coating of hydroxyapatite on their surface, increasing their bioactivity. The kind and concentration of bioactive elements, such as calcium (CaO) and phosphorus (P_2O_5), included into the glass structure, have an impact on the biodegradation rate. The bio-mineralization of glasses depends on the glass dissolving in contact with bodily fluids and the release of Ca and P ions. The connectivity of the glass network is generally lower for sol-gel-derived glasses than for melt-derived glasses. Modifier cations (Ca) reduce network connectivity, leading to faster degradation as CaO content increases. A reduction in Ca/P ratio leads to less significant degradation for materials with both CaO and P_2O_5 *(Schumacher et al., 2021)*. Bioactive glasses' surface properties and shape are extremely important to how quickly they degrade. Due to increased surface interactions with the environment, a bigger surface area encourages faster degradation. By aiding the flow of ions and water into the material, mesoporous or nanopores within the glass structure can further speed up degradation. By precisely controlling these variables, the sol-gel approach enables the production of bioactive glasses with different surface properties and morphologies. The surrounding environment, in particular the pH, temperature, and ion content, has an impact on how bioactive glasses degrade as well *(Schumacher et al., 2021).*

The biodegradability of bioactive glasses can be evaluated using a wide variety of methodologies and approaches. Gaining a thorough understanding of the kinetics and mechanism of degradation through the combination of several characterization techniques would help in the rational design and engineering of bioactive glass-based materials for a variety of biological applications. It has been established that the primary agents responsible for activating genes and so fostering a favorable gene response, which is directly related to the osteogenesis process, are ionic dissolution products *(Baino et al., 2018)*. One of the easiest and most popular ways to gauge the deterioration of bioactive glasses is mass loss. Glass samples are submerged in a physiological solution such as body fluids (SBF), tris buffer solution, phosphate buffered saline, and culture media for a predetermined amount of time, and weight loss is then calculated *(Tainio et al., 2017).* The ion release profile and pH change that occur during the breakdown of bioactive glasses can also reveal crucial details regarding the reaction kinetics and mechanism. Monitoring the basicity or acidity of the degradation media allows for the measurement of pH change *(Sanz-Herrera & Boccaccini, 2011).* Numerous research has examined the degrading behavior of bioactive glasses and discovered that the degradation rate may be controlled by modifying a variety of parameters, including the composition, surface characteristics, shape and environment.

2.6 Surfactants

According to a study by *(Baumard, 2005),* bioactive glass dissolution products allow the genes that control osteogenesis and the generation of growth factors to express themselves quickly. These findings have sparked in-depth research in to use of bioactive glass as tissue engineering scaffold. These qualities, along with a network of linked macrospores (with pore widths more than 100m) to allow for tissue ingrowth and nutrient delivery to the center of the regenerated tissue and a surface texture that encourages cell attachment, make up an ideal scaffold. The scaffold should be constructed using a processing method that can produce irregular shapes to match the deficiency in the patient's bone and be resorbable at controlled rates.

The interconnectedness, form and size distribution of the pores are only a few of the characteristics taken into account when describing the porosity *(Lutzweiler et al., 2020; Miao & Sun, 2009).* Since porosity characteristics are crucial in determining the entity of the interactions with cells and the environment as well as the drug release kinetics if controlled drug delivery from the mesoporous is the goal *(Adepu & Ramakrishna, 2021; Moritz & Geszke-Moritz, 2022).* Controlling pore

structure and size is essential for the production of substitutes for living tissues. Since it results directly from the synthesis process, the porosity structure is a fundamental property of sol-gel materials *(Baino et al., 2018).* The IUPAC system divides porous materials into three categories; macroporous materials, which have pores larger than 50 nm, mesoporous materials that have 2-50nm and microporous materials, with pores size less than 2 nm *(Thommes et al., 2015).*

Recent research has demonstrated that altering the glass surface property can enhance the kinetics of hydroxyapatite (HAp) deposition on the surface of BGs and their ability to bind tissues *(Migneco et al., 2020).* The creation of mesoporous bioactive glasses with a composition equivalent to that of regular glasses but with the benefits of an ordered mesoporous configuration is made possible by the employment of surfactants in sol-gel procedures. The bioactive glasses can have their bioactivity and biodegradability improved by this structured mesoporous structure, which makes them more useful for tissue engineering applications *(de Barros Coelho & Magalhães Pereira, 2005; Migneco et al., 2020).* Surfactants enable the synthesis of mesoporous bioactive glasses with a high specific surface area, which is necessary for achieving increases bioactivity, in sol-gel procedures *(S.-J. Shih et al., 2016).* After being submerged in simulated bodily fluid (SBF), the surfactants' ordered mesoporous structure improves the bioactivity of the glasses and encourages the development of hydroxyapatite (HAp) *(Aneb et al., 2023; S.-J. Shih et al., 2016).* Bioactive glasses' pore structure and surface characteristics can be affected by surfactants, which in turn affects how well the materials interact with cell and tissues. Through their impact on the pore structure and surface characteristics of the materials, surfactants have the ability to regulate the kinetics of degradation of bioactive glasses. Surfactants in the sol-gel synthesis procedure can control the release of ions and the production of calcium phosphates, which are critical for the bioactivity and degradation of the glasses *(de Barros Coelho & Magalhães Pereira, 2005; S.-J. Shih et al., 2016).*

Numerous surfactants have been researched for this reason because the type of surfactant selected can significantly affect the characteristics of the bioactive glass. A study by *(Schmitz et al., 2020)* showed that due to their lack of charge, non-ionic surfactants are less likely to interact with other charged species in a sol-gel system. Although non-ionic surfactants can also be utilized to construct mesoporous structures in bioactive glasses, the pore structure that results could be less organized *(Letaïef et al., 2014; Nejati Rad et al., 2020).* Depending on their charge, ionic surfactants are

either cationic or anionic. Surfactants that are cationic are positively charged, whereas those that are anionic are negatively charged *(Schmitz et al., 2020).* When ionic surfactants are used in sol-gel synthesis, ordered mesoporous structures can be created as a result of the surfactant molecules' ability to self-organize into micelles and produce well-ordered mesoporous *(Nejati Rad et al., 2020).* However, this structural agents are used at higher concentration in order to increase the SSA of the BG but this increases the aggregation and carbon contamination which leads to lowering the biocompatibility of the BG *(S.-J. Shih et al., 2016).* And some other surfactant such as hydrogen peroxide showed lower SSA *(Aklilu et al., 2023).* Bioactive glasses with better biological activities have been created using cationic surfactants, such as CTAB (cetyltrimethylammonium bromide). On the other hand, anionic surfactants have been used to improve the stability and dispensability of bioactive glass nanoparticles in aqueous solutions *(Baino et al., 2018).* The use of CTAB during the synthesis of bioactive glasses produce spherical particles that display a mesoporous and uniform surface. At lower pH value, the reaction favors a spherical shape due to the presence of cationic surfactant. This may be due to the dynamics of the CTAB micelles. Previous research by *(Letaïef et al., 2014),* has shown that micelles grow simultaneously with the formation of silica walls around them. In the case of bioactive glasses with ionic surfactants low pH value results in a slower polycondensetion process for the silica walls. These means that the lifetime of the micelles is similar to the at which the silica walls are being formed when the pH in the range of 3-5 *(Sierra et al., 2000).* As a result, well defined spherical particles are obtained. However, when the non-ionic surfactant is used to synthesis bioactive glasses, the ability of the nanoparticles to coalesce and form well defined individual particles decreases. These is because of the very low pH value, caused by the high acidity which leads to a slow growth of silica. As a result, the lifetime of the micelles becomes too short compared to the time required for the construction of silica walls around them. Consequently, the formation of the solid is not controlled by well-defined micelles.

In conclusion, because they are charged, ionic surfactants can help create ordered mesoporous structures and have a greater influence on the bioactivity and biocompatibility of bioactive glasses when used at lower concentrations. On the other hand, non-ionic surfactants have a lower propensity to interact with other charged species and may lead to less organized pore structure.

2.7 Research Gap

In majority of researches melt-quench is used as a synthesis method for bioactive glasses. However, the precursor materials are heated to high temperatures during the melt-quench technique which causes the production of undesirable crystalline phases and the loss of volatile substance. Rather, the sol-gel method has improved composition control, product homogeneity and the potential to create glasses with a greater surface area and porosity. This sol-gel method uses structure directing agents in most researches for the production of bioactive glasses to increase their SSA but most of them could be toxic, results with lower SSA, and the non-ionic surfactants are less likely to interact with other charged species in a sol-gel system and they do not have the ability to form mesoporous structure with well-defined mesoporousity. However, CTAB favors the synthesis of bioactive glasses with enhanced properties, including high specific surface area, mesoporous structure which their individual crystallite boundaries are defined.

But in most studies CTAB is used with base catalysts and inorganic acids which have high and low pH value that slows down and speeds up the polycondensation of silica wall around CTAB molecules which both catalysts decrease the formation of a well-defined spherical particle with mesoporous structure and cause toxicity which lowers the biocompatibility of the bioactive glass. But the use of organic acids like citric acid with the CTAB in the sol-gel synthesis of bioactive glass makes it easier to form well defend spherical particles with mesoporous structure due the its pH value that makes the micelles lifetime and the silica wall's construction rate the same. These acid works well at low concentrations and produces little residuals that are easily removed at low temperatures which makes them biocompatible.

And in other studies, CTAB surfactant has been used in the synthesis of bioactive glass to increase the SSA, which have showed a better outcome. But in order to increase the SSA it is used at higher concentration in most studies which resulted in higher carbon content leading to lowering the biocompatibility. Therefore, the synthesis of bioactive glass using a cationic surfactant which is CTAB at lower concentration with an organic acid catalyst citric acid by a sol-gel synthesis method to investigate their bioactivity, biocompatibility and biodegradability together with the concentration impact of CTAB on these three properties was not studied. Therefore, these work is to examine the bioactivity, biocompatibility and biodegradability of bioactive glasses synthesized

using sol-gel method by lower concentration CTAB surfactant and citric acid catalyst together with the concentration impact of CTAB on the biological properties of the bioactive glass.

CHAPTER THREE

3. METHODOLOGY

3.1 Chemicals and materials

The materials used to synthesis the bioactive glass powders are aluminum foil, beaker, stirrer bar, hot plate, drying oven, mortar, furnace, glass bottles, water bath, plastic tubs, centrifuge and hydraulic press. And the chemicals Tetraethyl orthosilicate (TEOS, $Si(OC_2H_5)_4$) (India, 98%), Phosphoric acid (H_3PO_4) (Sigma-Aldrich, 98%), Calcium nitrate tetra hydrate ($Ca(NO_3)_2.4H_2O$) (Loba chemicals ,98%), Cetyltrimethyl ammonium bromide (CTAB) (India. 99%), Citric acid ($C_6H_8O_7$) (Loba chemicals, 99.5%), distilled water and Ethanol (Loba chemicals,96%) which are commercially available are used. Chemicals used for the synthesis of simulated body fluid (SBF) are Sodium chloride (NaCl) (India, 98%), Sodium bicarbonate ($NaHCO_3$) (India, 99%), Potassium chloride (KCl) (Sigma-Aldrich, 99%), Disodium hydrogen phosphate (Na_2HPO_4) (India, 99.5%), Magnesium chloride hexahydrate ($MgCl_2.6H_2O$) (India, 99%), Hydrochloric acid (HCl) (Alpha chemicals, 98%), Calcium chloride ($CaCl_2$) (Loba chemicals, 95%), Sodium sulphate (Na_2SO_4) (Loba chemicals, 99%), tris(hydroxymethyl)aminomethane (TRIS) [= (CH2OH)3CNH2] (India, 99%). And for the in-vitro biocompatibility test MTT assay 3-(4,5-dimethylthiazol2-yl)-2,5-diphenylte-trazolium bromide and dimethyl sulfoxide (DMSO) were used as received.

3.2 Synthesis of bioactive glass powders

In this paper the bioactive glass powder was prepared using sol gel process as reported with little modification *(Letaïef et al., 2014).* During the process tetraethyl orthosilicate (TEOS) as silica precursor, Calcium nitrate tetra hydrate (CN, $Ca(NO_3)_2.4H_2O$) as CaO source, Phosphoric acid (H_3PO_4) as P_2O_5 source, Cetyltrimethylammonium Bromide (CTAB) as structure directing agent and Citric Acid as an acid catalyst were used. The synthesized powders have a glass composition of mole percentage of, 60% SiO_2, 36% CaO, and 4% P_2O_5. The types of synthesized samples were, BG without CTAB, BG with 0.1 M of CTAB, BG with 0.3 M of CTAB and BG with 0.5 M of CTAB. To prepare 0.2 M precursor in 50 mL ethanol and distilled water solvents with 1:1 ratio, 0.3 M of citric acid was added in to the solvents mixture and stirred at room temperature to catalyze the hydrolysis reaction. Then CTAB depending on the type of sample prepared was added in to the solution and stirred untill it is fully dissolved. Based on their solubility 1.249 mL TEOS,

0.039 mL H_3PO_4 and 0.850 g CN were added in to the mixture in 10 minutes interval under continious stirring *(Durgalakshmi et al., 2020; El-Fiqi et al., 2012).* To create a homogenous solution, the precursor solutions were agitated with a magnetic stirrer for 3 hours at room temperature on a hot plate until it turned into transparent solution. Then the produced sol were put in to the oven at 60°C for 24 hours to undergo polycondensation and turn into a gel. After the gel formation the temperature was increased into 100°C for 3 hours in order to dry the forming gel. Based on the TGA results of the dried gel, the samples were calcined at 550°C for 2 hours to decompose any leftover precursor residues and solvents for higher biocompatibility *(Chitra et al., 2019).* Then, XRD, SEM, BET, EDS, TEM and FTIR were used to characterize the produced samples. The in-vitro bioativity and biodegradability were tested using SBF and for the in-vitro biocompatibility MTT assay was used.

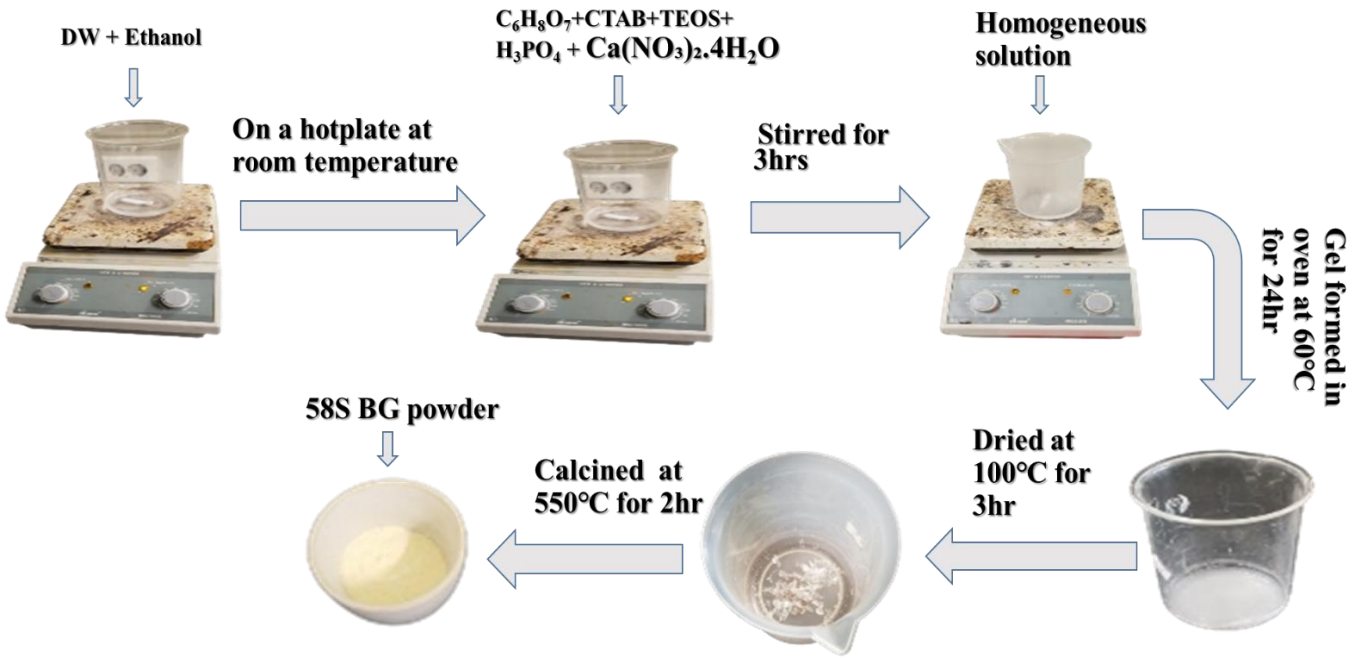

Figure 4. Synthesis of bioactive glass powders *(Letaïef et al., 2014).*

3.3 Preparation of simulated body fluid

Simulated body fluid (SBF) is a solution containing the same ionic concentration as the human body plasma as shown in table 1 *(Kokubo & Yamaguchi, 2019).* To prepare the SBF solution 6.54g sodium chloride (NaCl), 2.27g Sodium bicarbonate ($NaHCO_3$), 0.37g potassium chloride (KCl), 0.14g sodium dihydrogen phosphate (NaH_2PO_4) and 0.31g magnesium chloride hexahydrate ($MgCl_2.6H_2O$) were added to 1000ml distilled water and stirred on a hot plate at 37°C. Before adding the rest of the ions, a steady drop of 1M hydrochloric acid was added to the solution and then 0.37g of calcium dichloride ($CaCl_2$) and 0.071g of sodium sulfate (Na_2SO_4) were added. Lastly, to achieve a homogenous solution, it was stirred for 30 minutes after all the components were added and buffered at pH 7.4 using tris(hydroxymethyl)aminomethane (TRIS) maintaining the temperature at 37°C throughout *(Jang et al., 2018)*. In order to prevent the prepared solution from precipitating the solution was kept in a glass bottle in a regular refrigerator.

Table 1 Ion concentration of blood plasma and SBF *(Kokubo & Yamaguchi, 2019).*

Ions	Na^+	K^+	Mg^{2+}	Ca^{2+}	Cl^-	HCO^{3-}	HPO_4^{2-}	SO_4^{2-}	pH
Blood Plasma	142.0	5.0	1.5	2.5	103.0	27.0	1.0	0.5	7.2–7.4
Simulated body fluid (SBF)	142.0	5.0	1.5	2.5	147.8	4.2	1.0	0.5	7.4

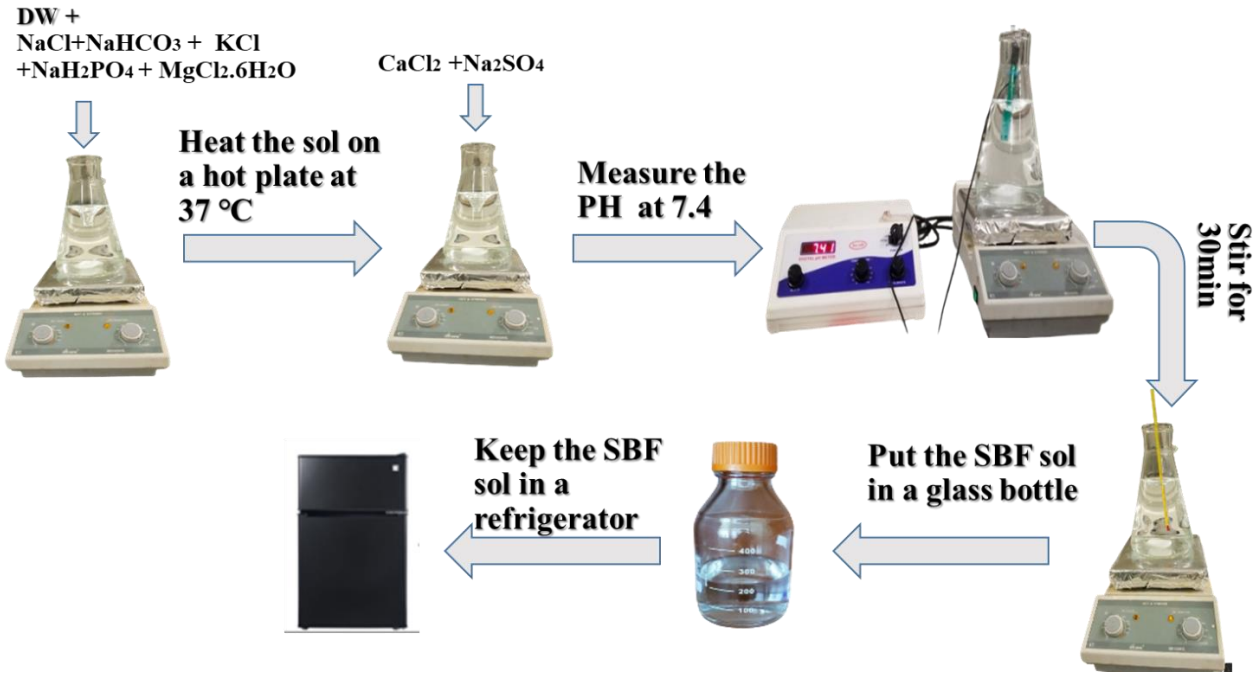

Figure 5. Procedure for the preparation of SBF *(Kokubo & Yamaguchi, 2019).*

.

3.4 Sample characterization

After sample preparation, Thermo gravimetric analysis (TGA)/Differential thermal analysis (DTA) (shimadzu DTG-60H) was used to confirm the temperature at which the BG powders are stabilized. X-ray diffraction (XRD) (Shimadzu XRD-7000) at copper Kα radiation (λCuKa=1.5418 Å) was used to characterize the phase composition of the BG samples. The functional groups of the BG powders were determined using Fourier transform infrared reflection (FTIR) (Perkin Elmer spectrum 65 FT-IR). The Scanning electron microscopy (SEM) (JSM 6500F JEOL) and Transition electron microscopy (TEM) (Tecnai G2 F20, Hillsboro) were used to observe the powder's surface morphologies. Selected area electron diffraction (SAED) (Tecnai G2 F20, Hillsboro) was used determine crystalline structure. Brunauer-Emmett-Teller (BET) (Novatouch 2LX) provided data on the specific surface area, pore volume and pore size of the BG powders. Energy dispersive x-ray spectroscopy (EDS) (JEOL Japan) determines chemical composition.

3.5 In-Vitro Bioactivity Test

In vitro bioactivity testing of all BG samples was conducted by immersing them in a solution having an ionic content similar to that of normal human plasma known as simulated body fluid (SBF). All sample powders were measured to 3 g and immersed in 10 mL, 15 mL and 12 mL of SBF. After being immersed in SBF, each sample was kept for 12 hours in a water bath that was kept at a steady 37°C. Then the immersed samples were washed three times in distilled water and dried for 24 hours at 80°C in an oven to characterize HAp formation using XRD for phase analysis, SEM determine surface morphology and FTIR to determine the functional group. After estimating the diffraction peak using the peak area analysis of HAp, the Debye-Scherer equation is used to calculate the bioactivity of each sample.

$$D = \frac{K\lambda}{\beta cos\theta}, \quad \text{.....1}$$

Figure 6. In vitro bioactivity test *(Chen et al., 2018; Letaïef et al., 2014).*

3.6 In-Vitro Biocompatibility Test

Utilizing the mouse preosteoblast cell line MC3T3-E1, the impact of CTAB and citric acid on 58S BG cell proliferation was investigated. In polystyrene plates enriched with α-MEM and supplemented with 10% fetal bovine serum (FBS) (Sigma-Aldrich, UK), 1% antibiotic, 2 mM glutamine and 0.1% penicillin streptomycin, the cells were seeded and allowed to attach. The seeded cells were cultured on a 24-well plate with at a density of 2×10^4 cells/cm^3. The sterile BGs powders using an autoclave and dispersed in minimum essential medium (MEM) at one of several extraction concentrations: 20%, 40%, 60%, 80% and 100% were introduced into direct contact with the cells once the cells reached confluence. The plates were then incubated at 37°C in a humid atmosphere with of 95% air and 5% CO_2 and incubated for 24 hours. Following the removal of the media, 300 µL of MTT reagent was added to each well, and the plates were incubated for 72 hours at 37°C in a CO_2 incubator. MTT is taken up by the cells through endocytosis and is enzymatically reduced by mitochondrial enzyme systems to insoluble formazan crystals *(Berridge et al., 2005).* Then the media containing MTT was removed and the formazan crystals were solubilized using solvent dimethyl sulfoxide (DMSO). The solubilized formazan dye results in colored solution which indicates the living cells. The optical density of the colored solution was then measured spectrophotometrically at wavelength of 570 nm. Then the cytotoxicity of the BG samples was determined by comparing absorbance values between control and experimental samples.

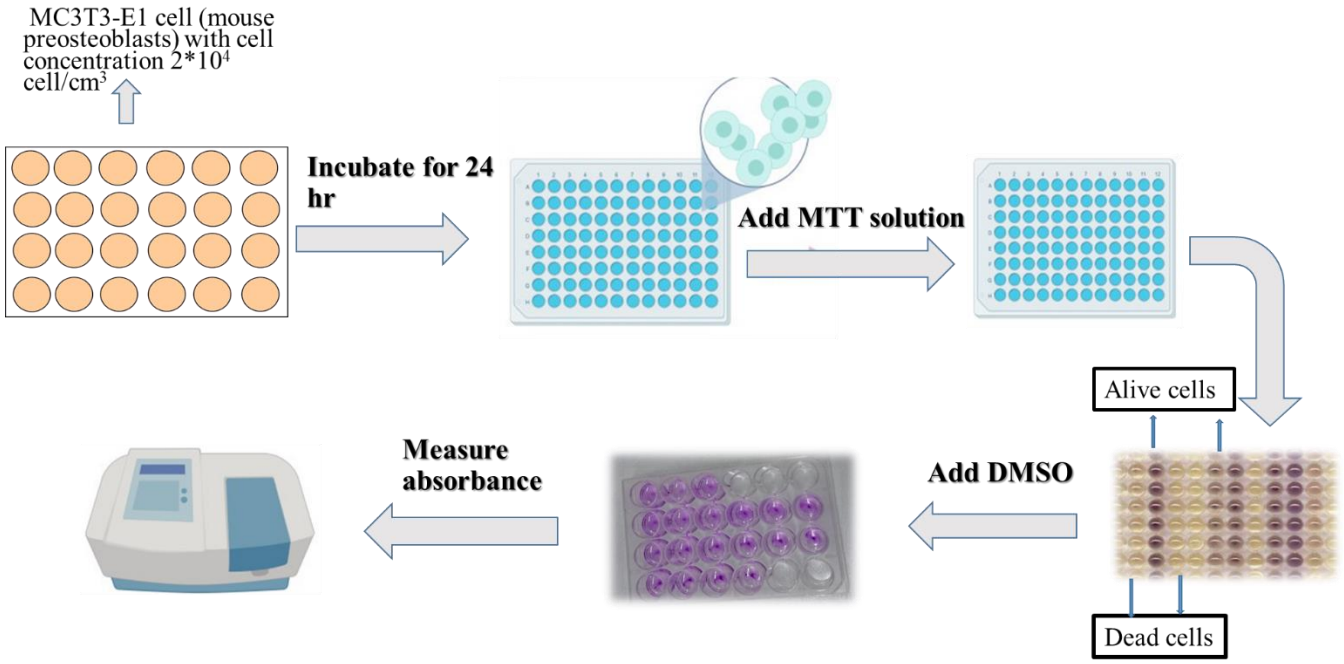

Figure 7. Procedure for in vitro biocompatibility test *(Siqueira et al., 2017).*

3.7 In-Vitro Biodegradability Test

The in vitro biodegradability test was conducted by soaking BG without CTAB (BG0), BG with 0.1 M of CTAB (BG1), BG with 0.3 M of CTAB (BG3) and BG with 0.5 M of CTAB (BG5) samples in SBF solution as pellet form. During the biodegradability test, pellets were employed for their convenient handling and accurate weight monitoring. As reported and with little modification, 6mm in diameter and 3.5mm thick BG tablets were prepared using hydraulic press with a load pressure of 15 MPa and a dwell time of 60 seconds. Three pellets were used per BG sample to determine the average and standard deviation of weight loss. The prepared pellets of each BG sample were immersed in SBF solution with a volume of 12ml which was conducted by using the formula (equation 2) according to mineralization experiment of international standards (ISO/FDIS 23317) *(Chen et al., 2018).*

$$\boldsymbol{Vs = \frac{Sa}{10}} \text{.....(2)}$$

The pellets soaked in the SBF solution were kept in a 37ºC water bath for 24 hours and dried at 80ºC for another 24 hours after being rinsed with ethanol and distilled water three times. Then the

weight of the BG pellets was measured in which the evaluation was conducted each day by replacing the SBF solution, drying the pellets and weighted for 30 days.

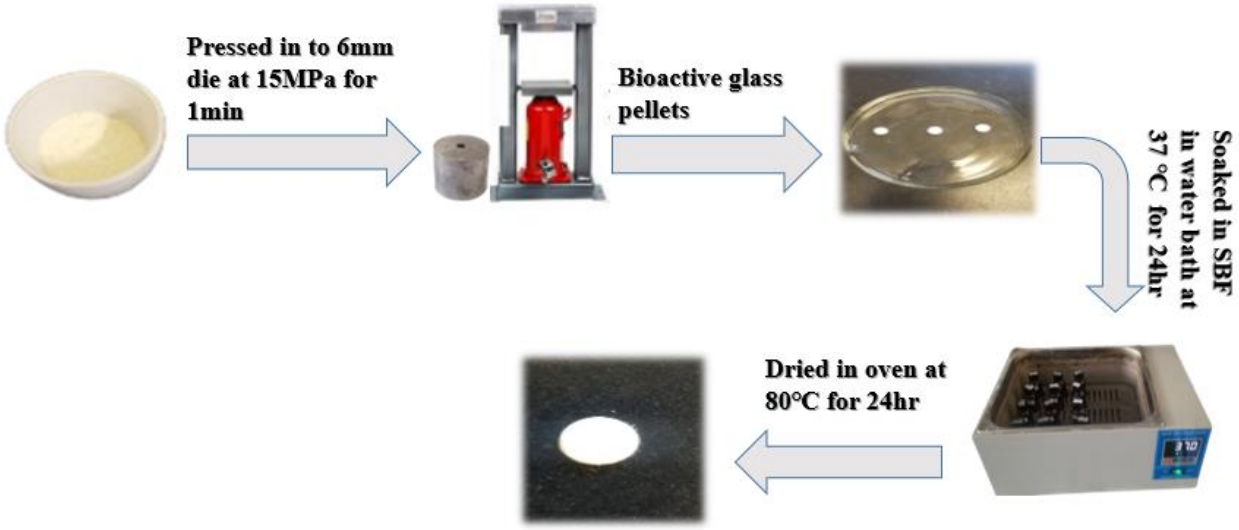

Figure 8. Procedure for in vitro biodegradability test *(Chen et al., 2018).*

CHAPTER FOUR

4. RESULTS AND DISCUSSION

The experimental was conducted to investigate the thermal stability, phase composition, chemical composition and particle morphology to determine the bioactivity, biocompatibility and biodegradability of the BGs.

4.1. Thermo-Gravimetric Analysis (TGA)

Figure 9 shows the TGA/DTA analysis with stabilization temperature for BG without CTAB (BG0), BG with 0.1 M of CTAB (BG1), BG with 0.3 M of CTAB (BG3) and BG with 0.5 M of CTAB (BG5) by heating the samples at a rate of 15 °C/min from 0-900 °C. All BG powders showed two main weight loss stages. The first weight loss of BG0, BG1 BG3 and BG5 during the temperature range from 200-350 °C were 53.785%, 46.129%, 87.249% and 58.632% respectively. The removal of water and alcohol residue that was left behind after drying is what causes the weight reduction. From the DTA results of all BG samples weight loss caused by the removal of the water and the residuals of alcohol groups were indicated with the endothermic peak (Mukundan et al., 2013). For BG1, BG3 and BG5, the decomposition of CTAB occurred at 319 °C *(Akrity Anand et al., 2019).* Another weight loss happened between 350 °C and 500 °C for BG without CTAB (BG0), BG with 0.1 M of CTAB (BG1), BG with 0.3 M of CTAB (BG3) and BG with 0.5 M of CTAB (BG5) which was 0.032%, 0.742%, 8.573% and 14.624%, revealed by exothermic peak at 450 °C. These was the decomposition of the $Ca(NO_3)_2$ in to nitrogen oxide, oxygen, water, and CaO and the discharge of further precursor residuals *(Santos et al., 2016).* Thus, 550 °C was the sample's stabilization temperature since all residuals were removed below this temperature. It is stated that the lowest stabilization temperature yields the most bioactivity *(Jones et al., 2006; Xynos et al., 2001).*

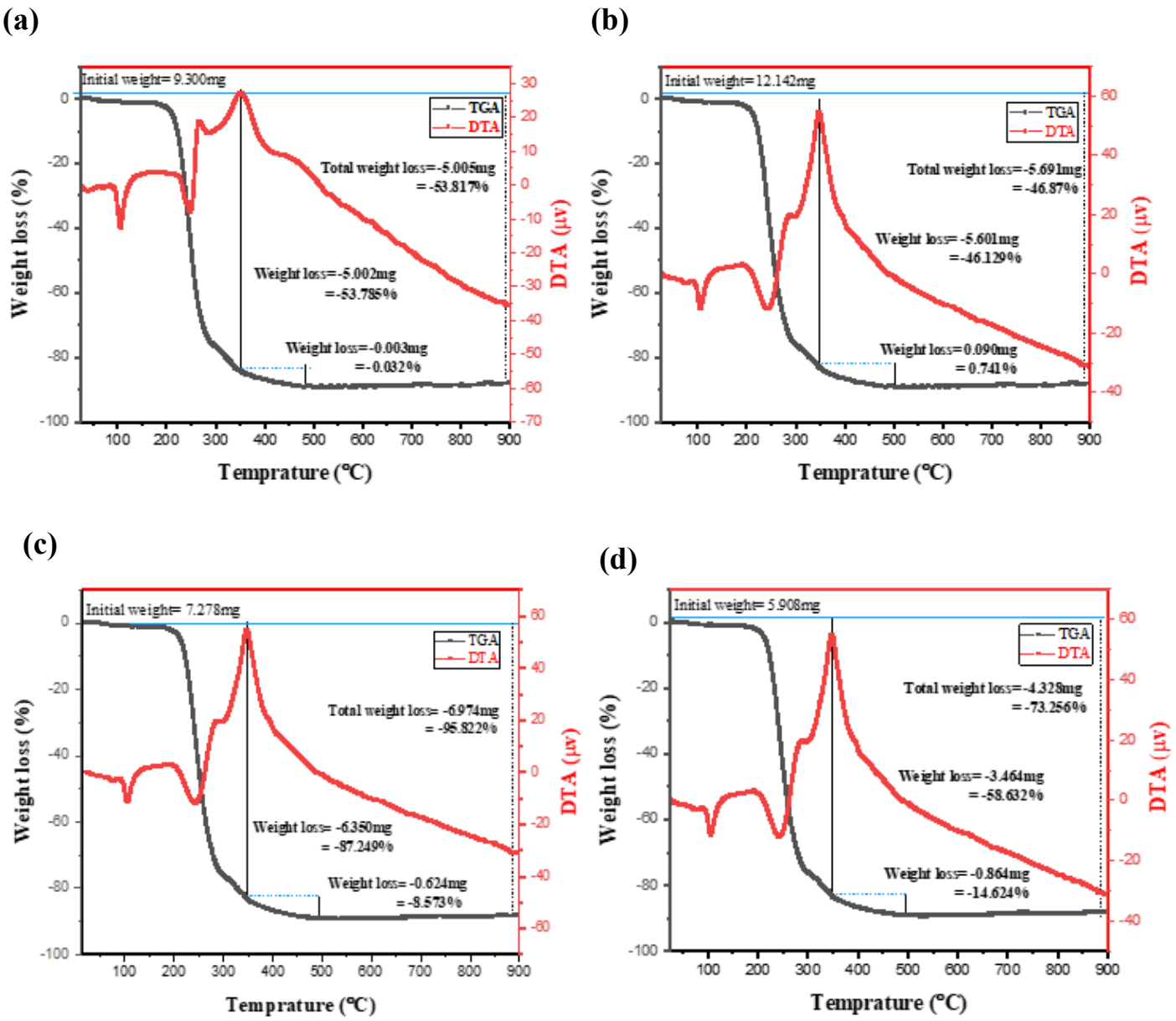

Figure 9. TGA and DTA analysis of BG without CTAB (BG0) (a), BG with 0.1 M of CTAB (BG1) (b), BG with 0.3 M of CTAB (BG3) (c) and BG with 0.5 M of CTAB (BG5) (d).

4.2. X-ray diffraction analysis (XRD)

The X-ray diffraction (XRD) pattern for each BG powders, BG without CTAB (BG0), BG with 0.1 M of CTAB (BG1), BG with 0.3 M CTAB (BG3) and BG with 0.5 M CTAB (BG5) calcined at 550 °C before soaking in SBF is shown in Figure 10. The powders exhibit atoms that lack a long-range order between 20° and 30º, which contributes to their amorphous nature *(Bento et al.*,

2021; Ravarian et al., 2010). It indicates that the atomic structure of the materials with and without the structural directing agent is not regular or recurring. Unlike crystalline materials, the arrangement of atoms in an amorphous material is chaotic *(Bento et al., 2021; Rezaei et al., 2014).* The absence of diffraction peaks on the pattern of the sample made with the ionic surfactant CTAB indicates that the mesoporous in this sample are not arranged in a periodic manner *(Letaïef et al., 2014).* Due to its absence of crystalline structure, glasses have special qualities like increased bioactivity and better dissolution rate which makes it dissolve more easily in bodily fluids and encourage the formation of new tissue *(Kaur et al., 2014).* Since BG's amorphous nature allows for the largest Si-OH group content which can be reached at a minimum stabilization temperature, it plays a significant role in reaching maximum bioactivity *(Houreh et al., 2017; Hsu et al., 2018; Kargozar et al., 2018).* Consequently, no distinct diffraction peaks were found, indicating that the BG particles remained amorphous at a calcination temperature of 550°C. It also indicates that the BG powders are free from impurities which is essential in biomedical applications.

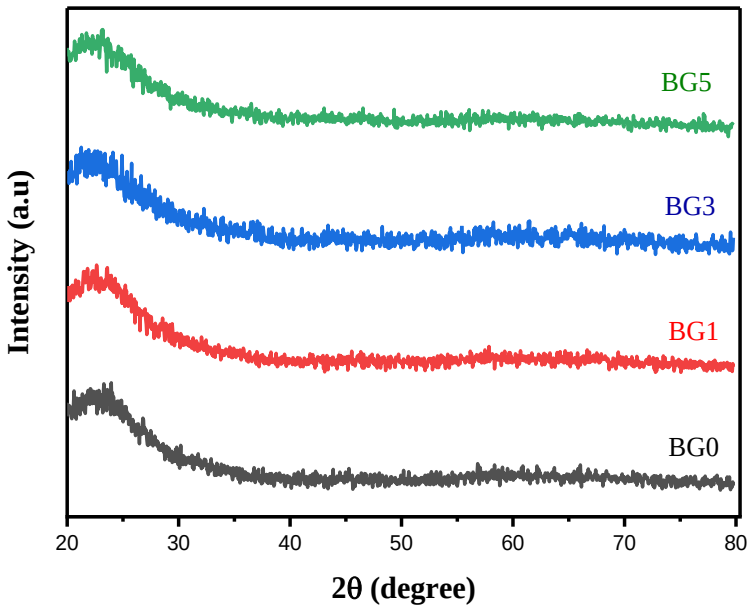

Figure 10. XRD patterns of BG without CTAB (BG0), BG with 0.1 M of CTAB (BG1), BG with 0.3 M of CTAB (BG3) and BG with 0.5 M (BG5) of CTAB before soaking in SBF.

4.3. Fourier Transform Infrared Spectroscopy (FTIR)

Figure 11 presents the FTIR spectra of the BG without CTAB (BG0), BG with 0.1 M of CTAB (BG1), BG with 0.3 M of CTAB (BG3) and BG with 0.5 M of CTAB (BG5) powders in the 500-4000 cm^{-1} spectral range before soaking in the SBF. All powders exhibited peaks associated with Si-O-Si symmetric stretching of bridging oxygen atoms assigned at 3448cm^{-1} and bending mode at 474 $cm^{-1,}$ 1078cm^{-1}, 1391cm^{-1} and 1650cm^{-1} *(ElBatal et al., 2003)*. The FTIR band at 958cm^{-1} presents Si-O-NBO which is mostly found at 940-1040cm^{-1} *(Balamurugan et al., 2006; Serra et al., 2003)*. The non-bridging oxygen indicates the modification of the glass network by a network modifier causing the part of Si-O-Si bonds to break. The decrease in silica network symmetry is caused by the addition of Ca^{2+} ion in the glass structure in which this non-bridging oxygen formation facilitates the dissolution of silica by forming silanol after soaking in SBF *(Aguiar et al., 2009; Barrioni et al., 2018)*. The peak at 1238cm^{-1} is not related to the formation of HAp, it is related to the presence of PO^{3-}_4 group within the glass structure *(Letaïef et al., 2014).*

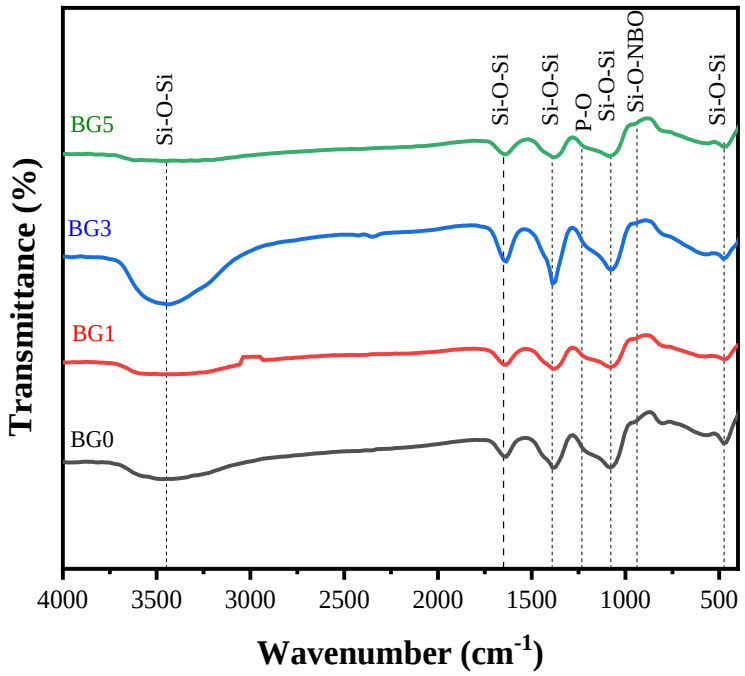

Figure 11. FT-IR spectra of BG without CTAB (BG0), with 0.1M of CTAB (BG1), with 0.3M of CTAB (BG3) and with 0.5M of CTAB (BG5) before soaking in SBF.

4.4. Scanning Electron Microscope (SEM)

Figure 12 shows the surface morphologies of all BG powders, BG without CTAB, BG with 0.1M of CTAB, BG with 0.3M of CTAB and BG with 0.5M of CTAB before soaking in SBF. As shown in Figure 12(a-d), all BG powder's particles have a smooth surface due to the presence of citric acid *(Lei et al., 2011)*. When bioactive glass is synthesized with CTAB, spherical particles with a smooth look are produced *(Letaïef et al., 2014)*. It appears that the cationic surfactant present in the reaction at lower pH caused by the addition of citric acid for the hydrolysis and condensation reaction promoted the formation of spherical shape which is related to the surfactant micelles interaction. Since the micelles must develop concurrently with the construction of the silica walls enclosing them to obtain controlled and well defined spherical particles, the lowest pH value of the citric acid with the cationic surfactant (CTAB) case resulted in a slower degree of polycondensation for the silica that forms the walls making the micelle's lifetime and the silica wall's construction rate the same *(Sierra et al., 2000)*. And this micelles formation prevents aggregation of particles *(Arsene et al., 2021)*. Micelles are aggregates of structural directing agent molecules *(Arsene et al., 2021)*. Therefore, more micelles form when the concentration of CTAB rises and these micelles have the ability to adsorb onto the surface of the bioactive glass particles resulting in aggregation of the CTAB molecules and form particles aggregation when CTAB is removed after calcination *(Lemyre & Ritcey, 2010)*. According to the SEM result BG with 0.5M of CTAB showed large aggregation of particles.

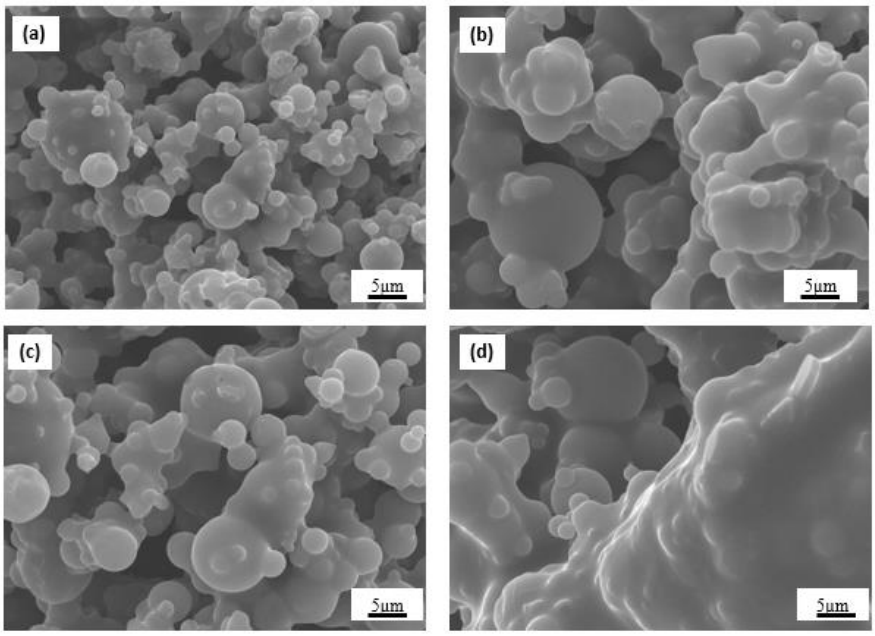

Figure 12. SEM images of BG samples without CTAB (BG0) (a), with 0.1M of CTAB (BG1) (b), with 0.3M of CTAB (BG3) (c) and with 0.5M of CTAB (BG5) (d) before soaking in SBF.

4.5 Brunauer-Emmett-Teller (BET) analysis

Specific surface area, pore volume and pore size were measured using the BET analysis as summarized in Table 2 for the BG without CTAB (BG0), BG with 0.1M CTAB (BG1), BG with 0.3M of CTAB (BG3) and BG with 0.5M of CTAB (BG5). Additionally, the P value difference between the BG samples indicating the important distinction within the samples resulted in $P<0.005$ and the standard deviation of n=3 are also shown in the table.

Table 2 Specific surface area, pore volume and pore size of BG without CTAB, with 0.1M, 0.3M and 0.5M CTAB.

Sample	Surface area (m^2/g)	P value	Pore volume (cc/g)	P value	Pore radius (nm)	P value
BG0	108.306±1.86	0.029	0.151±0.008	0.037	1.807±0.004	0.005
BG1	164.78±4.804	0.049	0.185±0.009	0.039	1.856±0.006	0.008
BG3	274.906±6.166	0.038	0.198±0.01	0.043	1.97±0.012	0.015
BG5	198.499±1.952	0.017	0.188±0.0098	0.042	1.869±0.01	0.013

4.5.1 Specific surface area, pore volume and pore size

From the BET analysis as shown in Table 2, the specific surface areas of BG without CTAB (BG0), BG with 0.1M CTAB (BG1), BG with 0.3M of CTAB (BG3) and BG with 0.5M of CTAB (BG5) were 108.306 ±1.86, 164.78 ±4.804, 274.906 ±6.166 and 198.499 ±1.952(m^2/g). The pore volume of the BG powders analyzed using BET were 0.151±0.008, 0.185±0.009, 0.198±0.01 and 0.188±0.0098(cc/g). And the pore sizes were 1.807±0.004, 1.856±0.006, 1.97±0.012 and 1.869±0.01(nm). According to the result shown in Figure 13(a and b), the specific surface area, pore volume and pore size increased as the concentration of CTAB increased from 0 to 0.3M. The increased values in SSA of the BG1 and BG3 compared to BG0 is due to the formation of the mesoporous structure which was obtained after the decomposition of CTAB during the heating process which was also confirmed by the TEM image on Figure 14. As shown on Table 2, BG3 has the highest SSA due to its high pore volume and size which is the result of the absence of aggregation as shown on the SEM image (Figure 12). However, the BG powder with 0.5M of CTAB showed decreased SSA compared to BG3. These is due to the rise in micelles formation of CTAB molecules in the solution in which these micelles are aggregates of the structural directing agent molecules *(Arsene et al., 2021).* Therefore, more micelles form when the concentration of CTAB rises and these micelles have the ability to adsorb on to the surface of the bioactive glass particles. The bioactive glass particles' surface area that is available for interactions with the environment is reduced as a result of these adsorption leading to lower formation of HAp resulting a decrease in the bioactivity of the BG. The increase in micelles formation also leads to a denser packing of structural directing agent molecules which the BG particles shrinks after the removal of CTAB resulting in smaller pore volume and pore size within the BG *(Lemyre & Ritcey, 2010).* These decreases the biodegradability of the BGs leading lower bioactivity.

Therefore, BG with 0.3M of CTAB showed better bioactivity and degradation rate compared to the other BGs due to the increased specific surface area which was obtained by the high pore volume and pore size formation within the BG which promotes appropriate ion release mechanism for the HAp formation.

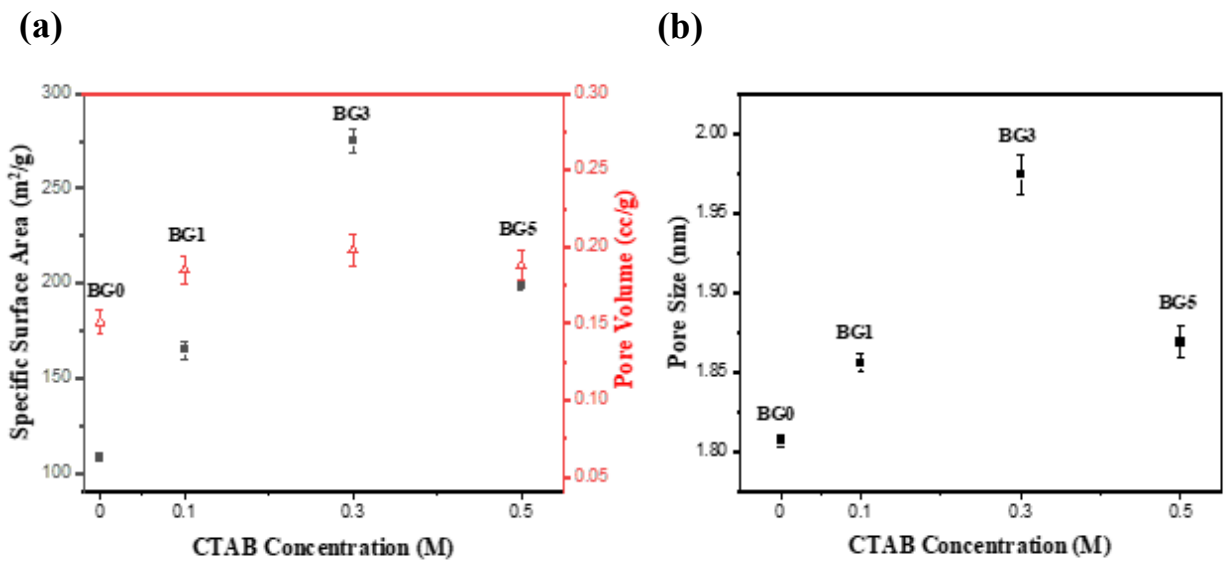

Figure 13. Specific surface area and pore volume (a) and pore size (b) of of BG without CTAB (BG0), BG with 0.1M of CTAB (BG1), BG with 0.3M of CTAB (BG3) and BG with 0.5M of CTAB (BG5).

4.6 Transmission Electron Microscope (TEM)

Figure 14 (a and b) shows the transmission electron micrographs of the BG powder without CTAB (BG0) and BG with 0.3M of CTAB (BG3). The highly formation of spherical particles and porous structure are seen in the TEM image of the BG3 inner region of the matrix Figure 14(b), which has a mesoporous pore volume and pore radius of 0.198±0.01and 1.97±0.012 as shown in Table 2. The pore volume and pore size of the BG increases as the concentration of CTAB increases up to BG powder with 0.3M of CTAB but start to decrease as the concentration increases further. An increase in pore volume and size is attributed to the formation of more CTAB micelle aggregates enveloped by BG precursors during the hydrolysis and condensation reactions, which create pores upon CTAB removal. As the CTAB concentration surpasses the optimal one (BG with 0.3M CTAB), the particles begin to aggregate due to the adsorption of CTAB clusters on their surfaces, leading to shrinkage, and a decrease in pore volume and size upon CTAB removal *(Lemyre & Ritcey, 2010)*. As shown in the high resolution TEM image, no crystalline grain boundaries were found due to the BG samples amorphous nature which was also confirmed by the SAED image shown on Figure 14(c), in which it was observed that the selected area diffraction image did not

show well defined ring *(S. J. Shih et al., 2016)*. The contrasts in brightness and darkness in the images reflect the varying thicknesses of particle walls and pores *(Hong & Shih, 2017)*. BG without CTAB (BG0) showed only thicker (darker) region indicating solid surface or absence of porous structure as illustrated on Figure 14(a). In Figure 14(b), BG3 showed thicker (darker) and thinner (brighter) regions which indicates the particle wall and pores revealing individual crystallites in spherical shape with mesoporous structure inside. Since pore volume and size, and specific surface area are directly related to bioactivity and biodegradability of BGs *(Xia & Chang, 2006)*, it was observed that BG with 0.3M of CTAB (BG3) has highest bioactivity and biodegradability due to the increased pore volume and pore size resulting in increased specific surface area which enables good formation of HAp layer on BG surface.

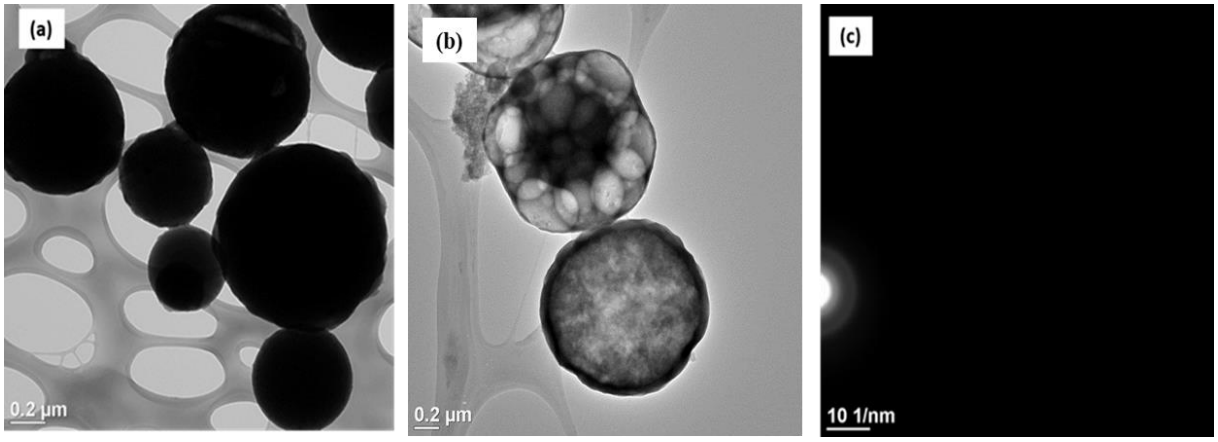

Figure 14. TEM image of BG without CTAB (BG0) (a), BG with 0.3M of CTAB (BG3) (b) and SAED image of BG with 0.3M of CTAB (BG3) (c).

4.7 Energy Dispersive X-ray Spectroscopy (EDS)

Figure 15 shows the EDS spectra of BG without CTAB (BG0) and BG with 0.3M of CTAB (BG3). The result indicated that the BG powders contain all the BG components Si, Ca and P indicating that there was no change in composition during the synthesis of the BG. it also indicated that the addition of CTAB and the concentration difference in the BGs did not influence the composition of the BG. Additionally, the result shows the successful formation of pores due to the removal of the organic residual (CTAB) during heating process which is reviled by the absence of the residual peaks. Biocompatibility of the BG samples was also indicated in these result due to the absence of carbon peak which could have been introduced by the CTAB.

(a) **(b)**

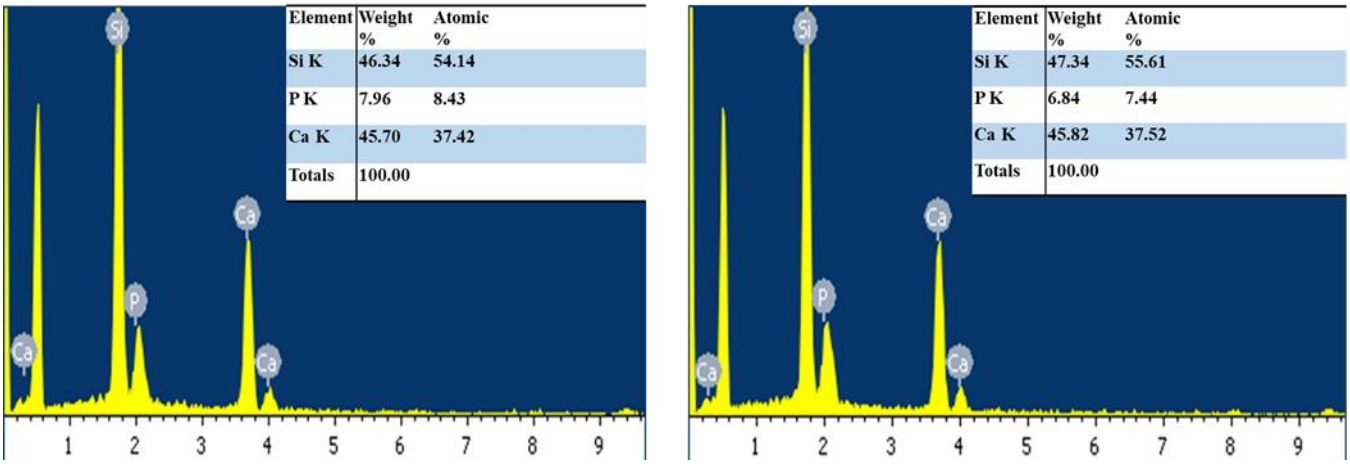

Figure 15. EDS analysis of (a)BG without CTAB (BG0) and (b) BG with 0.3M of CTAB (BG3).

4.8 In vitro bioactivity tests

4.8.1 X-ray diffraction analysis

The crystalline HAp layer formation after soaking in SBF for 12h was confirmed by XRD analysis as shown on Figure 16 for BG without CTAB (BG0), BG with 0.1M of CTAB (BG1), BG with 0.3M of CTAB (BG3) and BG with 0.5M of CTAB (BG5). Two main peaks of HAp phase reflection (JCPDS No. 00-009-0432) (002) and (211) appeared at 25.83° and 31.83°, and week peaks were also observed at 46.66° and 49.48° corresponding to the (312) and (213) reflections of HAp *(Sathiskumar et al., 2019)*. The presence of the HAp phase following immersion in SBF serves as an indicator of the bioactivity of the particles. A quicker appearance of the HAp phase is associated with increased rates of HAp formation and enhanced bioactivity. As shown on the result, the HAp phase was observed to form significantly earlier in the BG with 0.3M of CTAB (BG3) on the (312) and (213) after 12h of soaking in SBF compared to the other BG samples indicating that BG3 exhibit greatest bioactivity than BG0, BG1 and BG5. These is due to the observed largest surface area in BG3 which also indicates highest bioactivity as discussed on the BET analysis *(Xia & Chang, 2006)*.

The width of the XRD diffraction peak indicates the crystal size of the HAp layer, with broader peaks suggesting smaller or less perfect crystals *(Rezaei et al., 2014)*. As shown on Figure 16, BG with 0.3M of CTAB showed higher diffraction peak or intensity in which again corresponds to its

largest specific surface area compared to BG without CTAB, BG with 0.1M of CTAB, and BG with 0.5M of CTAB.

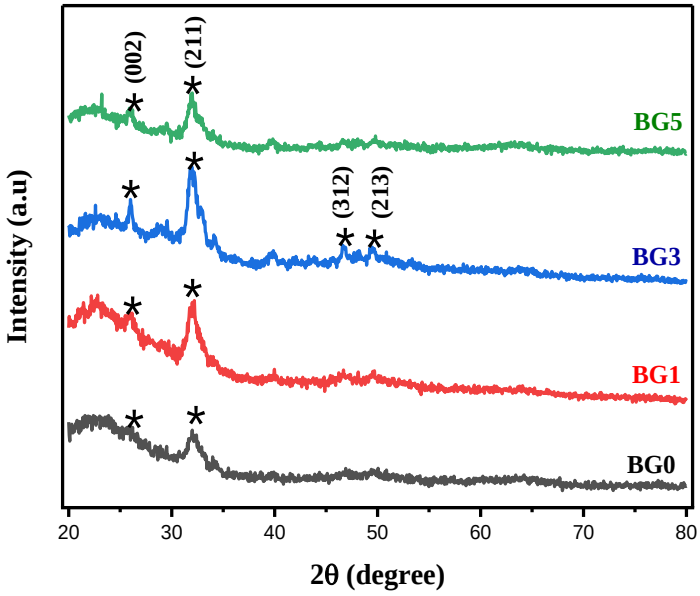

Figure 16. XRD patterns of BG without CTAB (BG0), with 0.1 M of CTAB (BG1), with 0.3 M of CTAB (BG3) and with 0.5 M of CTAB (BG5) after soaking in SBF for 12hr.

4.8.2 Bioactivity (crystallite size)

Figure 17 shows the bioactivity of BG without CATB, BG with 0.1M of CTAB (BG1), BG with 0.3M of CTAB (BG3) and BG with 0.5M of CTAB (BG5) after soaking in SBF for 12hr. The bioactivity of the BG samples was explained by the formation of HAp layer on their surface. To determine the bioactivity of BGs the crystallite size from the XRD pattern was calculated using Scherer formula (equation1). The crystalline size of BG without CATB (BG), BG with 0.1M of CTAB (BG1), BG with 0. 3M of CTAB (BG3) and BG with 0.5M of CTAB (BG5) after soaking in SBF for 12h were 0.32, 0.53, 3.09 and 0.56nm. The crystalline size increased as the concentration of CTAB increased as shown on Figure 17. Breakdown of silica network and ion exchange are the most crucial procedures to begin HAp layer growth. Hence, the BGs SSA has a significant impact on these process. The SSA increases as the CTAB concentration increases to some extent which was 0.3M due to its proper mesoporous structure formation as discussed on the

TEM (Figure 14(a and b)). Therefore, BG with 0.3M of CTAB (BG3) exhibited highest crystalline size indicating highest bioactivity compared to BG0 which had solid surface, BG1 with little pore formation and BG5 which showed lower pore formation due its aggregated particles caused by excess concentration of CTAB.

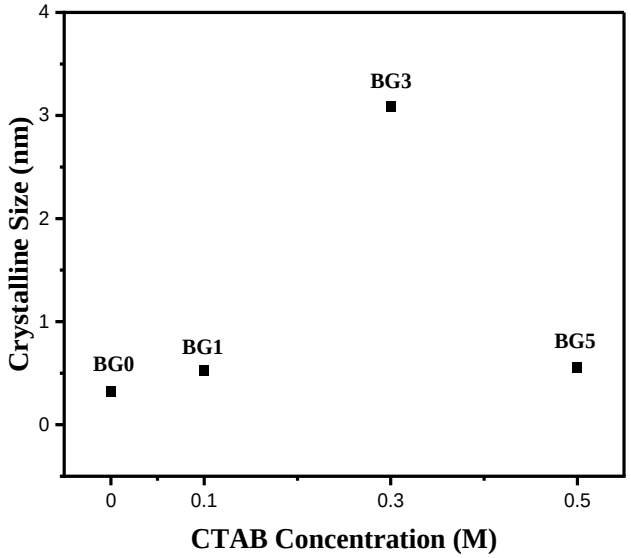

Figure 17. Crystalline size of BG without CTAB (BG0), with 0.1M of CTAB (BG1), with 0.3M of CTAB (BG3) and with 0.5M of CTAB (BG5) after soaking in SBF for 12hr.

4.8.3 Fourier transform infrared spectroscopy (FTIR)

Figure 18 shows the FTIR spectra of BG without CTAB (BG0), BG with 0.1M of CTAB (BG1), BG with 0.3M of CTAB (BG3) and BG with 0.5M of CTAB (BG5) in the range 500-4000cm^{-1} spectra after soaking in SBF for 12 hours. All samples exhibited bands of the silicate vibrations at 469.565, 1077.170, 1637.944, 3467.193cm-1, and non-bridging oxygen at 958.102cm-1 as shown on the figure. These NBO indicates the decrease in silica network symmetry due to the addition of network modifier ($Ca^{2+)}$ which facilitates the dissolution of the BG after soaking in SBF. The peak at 1238cm^{-1} is related to the presence of PO^{3-}_4 group within the glass structure, it is not related to HAp formation (Letaïef et al., 2014). The FTIR analysis showed additional new peaks at 562,

796.047 and 922.529cm-1 which were assigned to the crystalline P-O bands *(Min et al., 2016; Zhu et al., 2008).* These reveals the formation of crystalline HAp layer on the mesoporous BG surface after 12hr of soaking in SBF solution. The HAp crystalline layer formation indicates the bioactivity of the BG powders.

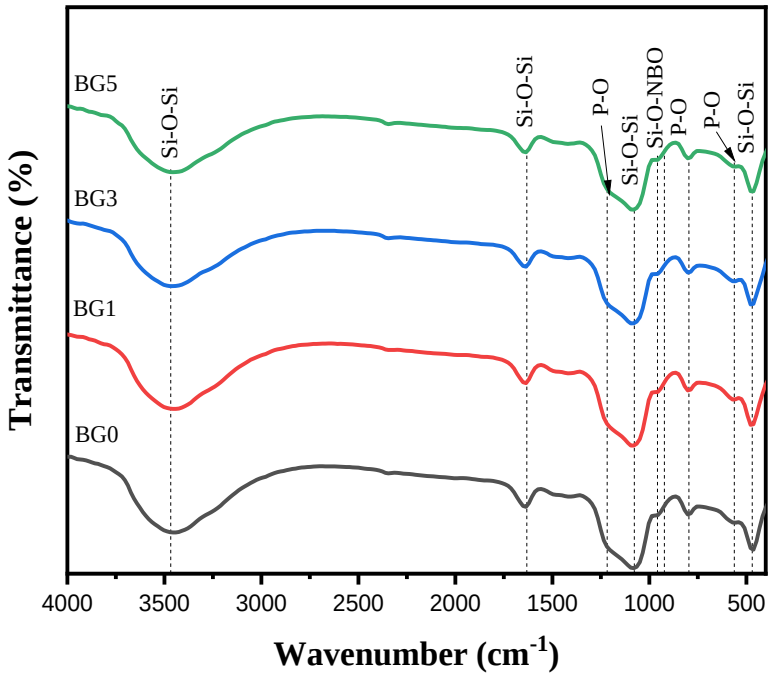

Figure 18. FT-IR spectra of BG without CTAB (BG0), with 0.1M of CTAB (BG1), with 0.3M of CTAB (BG3) and with 0.5M of CTAB (BG5) after soaking in SBF for 12hr.

4.8.4 Scanning electron microscope (SEM)

After soaking in SBF for 12hr, a change in the BG without CTAB (BG0), BG with 0.1M of CTAB (BG1), BG with 0.3M of CTAB (BG3) and BG with 0.5M of CTAB (BG5) surface morphology was observed as shown on Figure 19 in which these change is particularly formation of HAp layer. Flowery or needle like precipitates were shown on surface of all BG particles which completely covered the BG surface indicating formation of crystalline HAp layer as shown on Figure 19 *(Letaïef et al., 2014).*

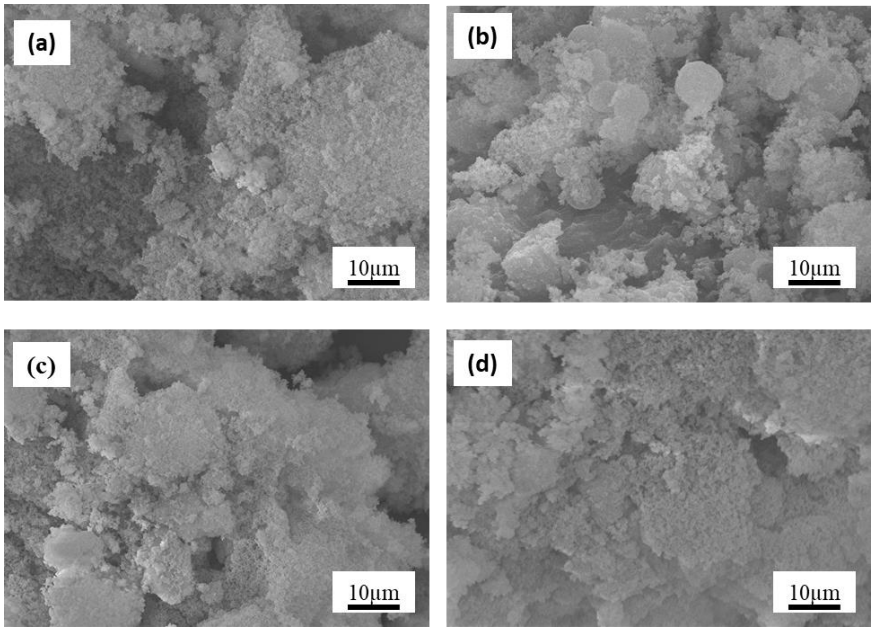

Figure 19. SEM images of BG samples BG without CTAB (BG0) (a), with 0.1M of CTAB (BG1) (b), with 0.3M of CTAB (BG3) (c) and with 0.5M of CTAB (BG5) (d) after soaking in SBF for 12hr.

4.9 Biocompatibility

Figure 20 shows the quantitative findings of the proliferation of the mouse preosteoblast cell line MC3T3-E1 on BG samples using 3-(4,5-dimethylthiazol-2-yl)-2,5-diphenyl tetrazolium bromide (MTT). BG nanoparticles were applied in different concentrations to the MC3T3-E1 pre-osteoblastic cells. A biocompatible material's cell viability should be at least 70% or above, in accordance with ISO 10993 standards *(Aklilu et al., 2023; Barrioni et al., 2019).* As shown on Figure 20, all samples showed cell viability of more than 70% which means BG without CTAB and BG with 0.1M, 0.3M and 0.5M concentration of CTAB were not toxic to the cell on the extraction concentration between 20% and 100%. Additionally, these confirms using CTAB at lower concentration results in a biocompatible BG due to the absence of the carbon contamination which could be caused by using CTAB at higher concentration.

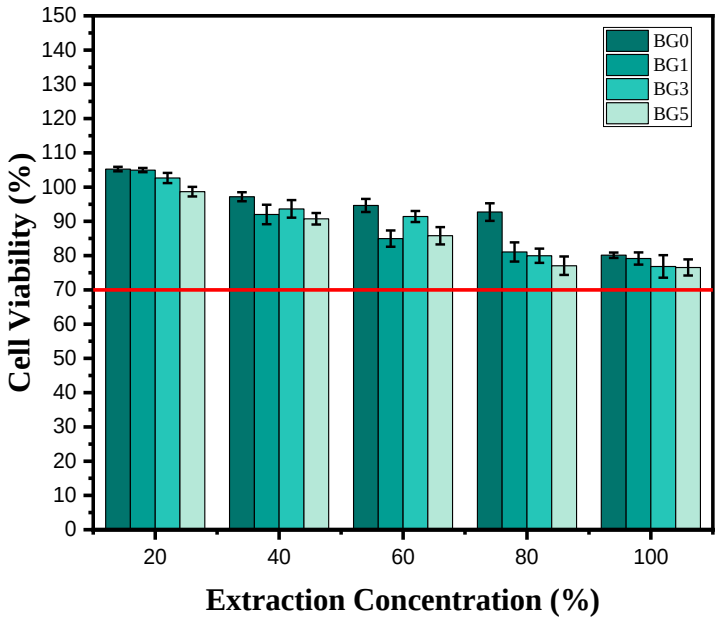

Figure 20. MTT analysis for cell viability of mouse preosteoblast cell line MC3T3-E1 treated with the cell culture medium containing BGs at different concentration.

4.10. Biodegradability

Figure 21 shows the weight loss of BG without CTAB (BG0), BG with 0.1M of CTAB (BG1), BG with 0.3M of CTAB (BG3) and BG with 0.5M of CTAB (BG5) after soaking in SBF. It illustrates the biodegradability property of the BG pellets which was conducted for 30 days. The BG pellets experienced weight loss of 5.22 ± 0.82, 17.82 ± 0.73, 35.53 ± 0.82 and 25.24 ± 0.55. The biodegradability of BGs significantly enhances their reactivity contributing to the formation of the HAp layer. As shown on the figure, BG without CTAB (BG0) showed lowest biodegradation due to its solid morphology which was also illustrated on the TEM image (Figure 14(a)). These lowers the dissolution of the BG particles due to its low SSA. Since BG with 0.1M of CTAB (BG1) showed higher SSA than BG0 as discussed on the BET analysis, the biodegradability BG1 was higher than BG0. BG with 0.3M of CTAB (BG3) showed highest weight loss compared to the rest of BG pellets due to its high mesoporous structure formation resulting in high SSA. The high SSA leads to a good interaction with the SBF and an easy dissolution of the ions to form HAp layer on the BG surface. These enables the BG to have a better degradation which also leads to a better bioactivity *(Bakare et al., 2019).* However, as

concentration of CTAB increases to 0.5M, the biodegradability of the BG decreased due to its low SSA which was caused by the aggregation of the particles.

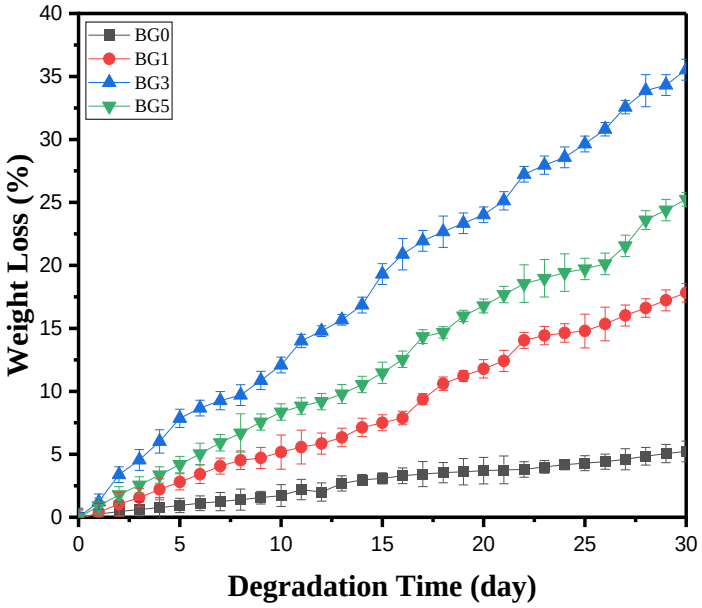

Figure 21. Weight loss of BG samples BG without CTAB (BG0), with 0.1M of CTAB (BG1) , with 0.3M of CTAB (BG3) and with 0.5M of CTAB (BG5) after soaking in SBF for 30 days.

4.10.1 Degradation rate Vs CTAB concentration and specific surface area

A bioactive glass should be able to promote the creation of the HAp layer and encourage to stimulate biological interaction by degrading at a suitable rate. With respect to CTAB concentration and SSA, Figure 22 shows the degradation rate of BG without CTAB (BG0), BG with 0.1M of CTAB (BG1), BG with 0.3M of CTAB (BG3) and BG with 0.5M of CTAB (BG5). For BG0, BG1, BG3 and BG5, the degradation rate was 0.17 ± 0.027, 0.59 ± 0.024, 1.18 ± 0.025 and 0.84± 0.018. Both the SSA of BG particles and the CTAB concentration have a significant impact on the degradation rate. Since it offers more sites for ion exchange and interactions with bodily fluids, a greater SSA might cause degradation more quickly by facilitating the development of HAp. These layer can operate as a barrier against further breakdown, coating the glass surface and slowing down the dissolution process *(Sanz-Herrera & Boccaccini, 2011)*. BG3 showed the highest degradation rate compared to B0, BG1 and BG5, and BG0 had the lowest degradation rate.

These is due to the difference in their SSA resulted from varying CTAB concentration which caused different surface morphologies. Hence, BG with 0.3M of CTAB (BG3) had the highest degradation rate due to its high SSA as shown on Figure 22.

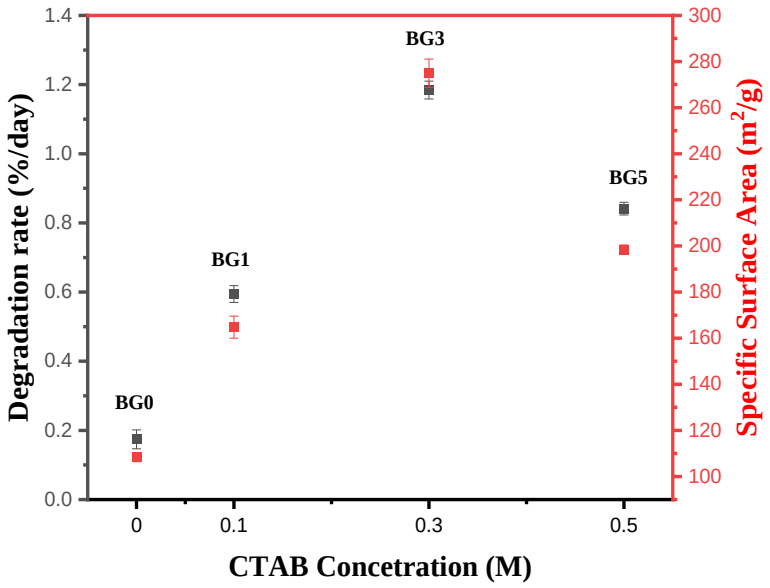

Figure 22. Degradation rate and specific surface area of BG without CTAB (BG0), with 0.1M of CTAB (BG1), with 0.3M of CTAB (BG3) and with 0.5M of CTAB (BG5).

4.11 Bioactivity and biodegradation correlation

Figure 23(a) shows the relation between bioactivity and degradation rate of BG without CTAB (BG0), BG with 0.1M of CTAB (BG1), BG with 0.3M of CTAB (BG3) and with 0.5M of CTAB (BG5). The bioactivity and biodegradability of the BG samples increased as the CTAB concentration increased from 0- 0.3M. These is due to an increase in formation of mesoporous structure which is caused by formation of more CTAB micelle aggregates surrounded by BG precursors during the hydrolysis and condensation reactions, which create mesoporous structure after CTAB removal. These increase in porosity leads to an increase in SSA indicating a better bioactivity and biodegradability of the BG which was also shown on Figure 23(b*) (Bakare et al., 2019).* BG with 0.3M of CTAB (BG3) showed high mesoporous structure formation leading to an increased SSA. Thus, BG3 exhibited highest bioactivity and biodegradability. However, as the

CTAB concentration increased to 0.5M, the particles begin to aggregate due to the adsorption of CTAB clusters on their surfaces, leading to shrinkage, and a decreased the porosity of the BG. Therefore, as shown on Figure 23(a), as the concentration of CTAB increased to 0.3M the bioactivity and biodegradability also increased, and as SSA increased so as the bioactivity and biodegradability as shown on Figure 23(b).

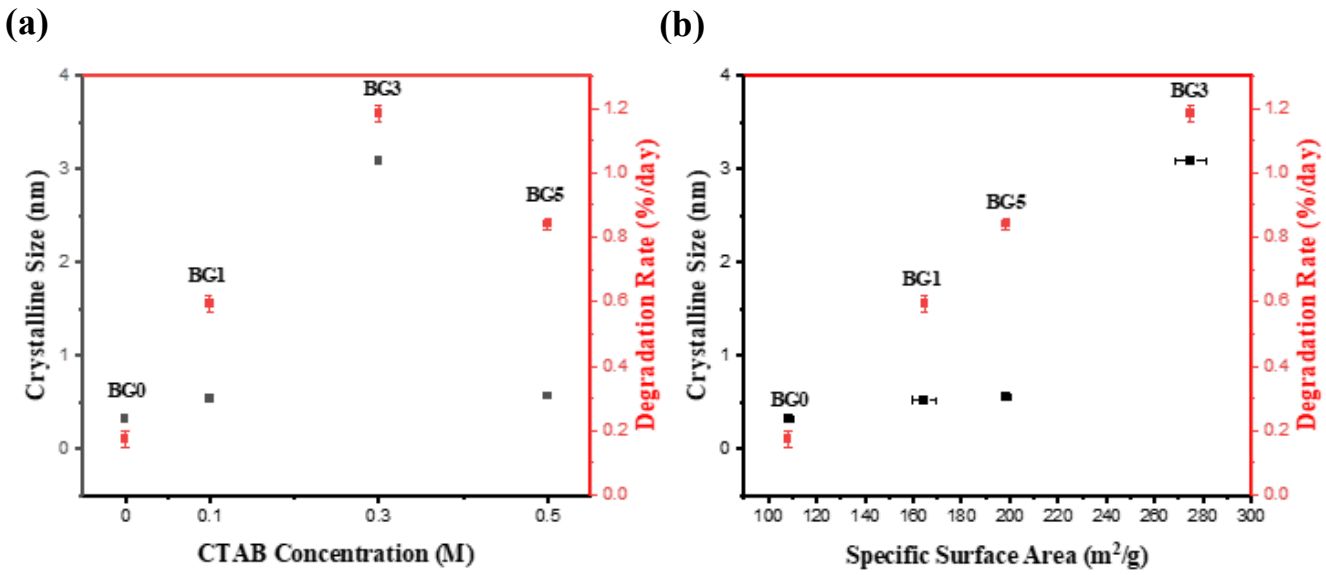

Figure 23. Correlation of crystalline size with degradation rate as a function of CTAB concentration (a) and as a function of specific surface area (b).

5. CONCLUSIONS and RECOMMENDATIONS

5.1 Conclusions

BG powders without CTAB (BG0), BG with 0.1M of CTAB (BG1), BG with 0.3M of CTAB (BG3) and BG with 0.5M of CTAB (BG5) were successfully synthesized utilizing the so-gel method in this study. A mesoporous bioactive glass with a composition of $60SiO_2$-$36CaO$-$4P_2O_5$ was synthesized employing low concentration CTAB structural directing agent, and the textural and structural properties of these glasses were studied. The bioactive glasses synthesized using the cationic surfactant obtained spherical mesoporous glass particles. The high specific surface area, pore volume and pore size of the mesoporous bioactive glass allowed for rapid ionic exchanges with the surrounded SBF solution, enhancing its bioactivity and biodegradability after soaking in SBF just for 12 hours. BG with 0.3 M of CTAB (BG3) showed highest specific surface area as shown on the BET study and showed highest production of crystalline HAp which was conducted using XRD, SEM and FTIR for the in-vitro bioactivity test. The results of the bioactivity and biodegradability tests showed a strong correlation between the bioactivity and specific surface area in which suggests that the larger specific surface area of the BG particles led to superior bioactivity and biodegradability of the BG. According to the MTT assay, all BG powders, containing CTAB with different concentration also showed a cell viability above 70%, which confirms the biocompatibility of the BGs. Therefore, BG with a better bioactivity and biodegradability in addition to biocompatibility was achieved by using CTAB surfactant at lower concentration with citric acid.

5.2 Recommendations

To achieve high SSA for a better bioactivity and biodegradability, various structural directing agents have been employed for the production of bioactive particles. This study found that CTAB with citric acid effectively form a spherical particle with well-defined mesoporous structure and was able to form biocompatible bioactive glasses. Despite the working environment and time, the characterizations essential findings yield viable recommendations. Such as, analyzing the released ion in the SBF solution after soaking the bioactive glass powders or pellets and in vivo biocompatibility tests analysis can expand opportunities for understanding the bioactive glass's properties for clinical use. These bioactive glasses can be expanded for drug delivery, wound healing and cancer treatment. implementing these suggestions will increase the medical development by a step.

6. REFERENCE

Adepu, S., & Ramakrishna, S. (2021). Controlled drug delivery systems: current status and future directions. *Molecules*, *26*(19), 5905.

Aguiar, H., Serra, J., González, P., & León, B. (2009). Structural study of sol–gel silicate glasses by IR and Raman spectroscopies. *Journal of Non-Crystalline Solids*, *355*(8), 475-480.

Aklilu, T. C., Ewnete, B. G., Dachasa, K., Sanbaba, K., Tesfaye, D., Wondimu, T. H., Kim, J. Y., Tulu, K. T., Lemma, S., & Ejeta, B. M. (2023). Citric Acid Catalyst-Assisted Bioactive Glass with Hydrogen Peroxide for In Vitro Bioactivity and Biodegradability Using Sol-Gel Method. *International Journal of Biomaterials*, *2023*(1), 9911205.

Al-Harbi, N., Mohammed, H., Al-Hadeethi, Y., Bakry, A. S., Umar, A., Hussein, M. A., Abbassy, M. A., Vaidya, K. G., Al Berakdar, G., & Mkawi, E. M. (2021). Silica-based bioactive glasses and their applications in hard tissue regeneration: A review. *Pharmaceuticals*, *14*(2), 75.

Amini, A. R., Laurencin Ct Fau - Nukavarapu, S. P., & Nukavarapu, S. P. Bone tissue engineering: recent advances and challenges. (0278-940X (Print)).

Anand, A., Lalzawmliana, V., Kumar, V., Das, P., Devi, K. B., Maji, A. K., Kundu, B., Roy, M., & Nandi, S. K. (2019). Preparation and in vivo biocompatibility studies of different mesoporous bioactive glasses. *J Mech Behav Biomed Mater*, *89*, 89-98. https://doi.org/10.1016/j.jmbbm.2018.09.024

Anand, A., Lalzawmliana, V., Kumar, V., Das, P., Devi, K. B., Maji, A. K., Kundu, B., Roy, M., & Nandi, S. K. (2019). Preparation and in vivo biocompatibility studies of different mesoporous bioactive glasses. *Journal of the Mechanical Behavior of Biomedical Materials*, *89*, 89-98.

Andersson, Ö., & Kangasniemi, I. (1991). Calcium phosphate formation at the surface of bioactive glass in vitro. *Journal of biomedical materials research*, *25*(8), 1019-1030.

Aneb, K., Oudadesse, H., Khireddine, H., Lefeuvre, B., Merdrignac-Conanec, O., Tessier, F., & Lucas, A. (2023). Study of the effect of ordered porosity and surface silanization on in vitro bioactivity of sol-gel-derived bioactive glasses. *Materials Today Communications*, *34*, 104992.

Arcos, D., Greenspan, D., & Vallet-Regi, M. (2002). Influence of the stabilization temperature on textural and structural features and ion release in SiO2− CaO− P2O5 Sol− Gel glasses. *Chemistry of Materials*, *14*(4), 1515-1522.

Arrington, E. D., Smith, W. J., Chambers, H. G., Bucknell, A. L., & Davino, N. A. (1996). Complications of Iliac Crest Bone Graft Harvesting. *Clinical Orthopaedics and Related Research (1976-2007)*, *329*, 300-309. https://journals.lww.com/corr/fulltext/1996/08000/complications_of_iliac_crest_bone_graft.37.aspx

Arsene, M.-L., Răut, I., Călin, M., Jecu, M.-L., Doni, M., & Gurban, A.-M. (2021). Versatility of reverse micelles: From biomimetic models to nano (bio) sensor design. *Processes*, *9*(2), 345.

Aurégan, J.-C., & Bégué, T. (2015). Bioactive glass for long bone infection: a systematic review. *Injury*, *46*, S3-S7. https://doi.org/https://doi.org/10.1016/S0020-1383(15)30048-6

Baino, F., Fiorilli, S., & Vitale-Brovarone, C. (2016). Bioactive glass-based materials with hierarchical porosity for medical applications: Review of recent advances. *Acta biomaterialia*, *42*, 18-32.

Baino, F., Fiume, E., Miola, M., & Verné, E. (2018). Bioactive sol-gel glasses: processing, properties, and applications. *International Journal of Applied Ceramic Technology*, *15*(4), 841-860.

Bakare, F. F., Chou, Y.-J., Huang, Y.-H., Tesfay, A. H., Moriga, T., & Shih, S.-J. (2019). Correlation of morphology and in-vitro degradation behavior of spray pyrolyzed bioactive glasses. *Materials*, *12*(22), 3703.

Balamurugan, A., Sockalingum, G., Michel, J., Fauré, J., Banchet, V., Wortham, L., Bouthors, S., Laurent-Maquin, D., & Balossier, G. (2006). Synthesis and characterisation of sol gel derived bioactive glass for biomedical applications. *Materials Letters*, *60*(29-30), 3752-3757.

Baldwin, P., Li, D. J., Auston, D. A., Mir, H. S., Yoon, R. S., & Koval, K. J. (2019). Autograft, Allograft, and Bone Graft Substitutes: Clinical Evidence and Indications for Use in the Setting of Orthopaedic Trauma Surgery. *Journal of Orthopaedic Trauma*, *33*(4), 203-213. https://doi.org/10.1097/bot.0000000000001420

Barone, A., Ricci, M., Mangano, F., & Covani, U. (2011). Morbidity associated with iliac crest harvesting in the treatment of maxillary and mandibular atrophies: a 10-year analysis. *Journal of oral and maxillofacial surgery*, *69*(9), 2298-2304.

Barrioni, B. R., de Laia, A. G. S., Valverde, T. M., da Mata Martins, T. M., Caliari, M. V., de Sa, M. A., de Goes, A. M., & de Magalhães Pereira, M. (2018). Evaluation of in vitro and in vivo biocompatibility and structure of cobalt-releasing sol-gel bioactive glass. *Ceramics International*, *44*(16), 20337-20347.

Barrioni, B. R., Norris, E., Li, S., Naruphontjirakul, P., Jones, J. R., & Pereira, M. d. M. (2019). Osteogenic potential of sol–gel bioactive glasses containing manganese. *Journal of Materials Science: Materials in Medicine*, *30*, 1-15.

Baumard, J. (2005). THE STORY OF BIOGLASS Larry HENCH Imperial College, London, UK.

Beaman, F. D., Bancroft, L. W., Peterson, J. J., & Kransdorf, M. J. (2006). Bone graft materials and synthetic substitutes. *Radiol Clin North Am*, *44*(3), 451-461. https://doi.org/10.1016/j.rcl.2006.01.001

Bellucci, D., Sola, A., Salvatori, R., Anesi, A., Chiarini, L., & Cannillo, V. (2017). Role of magnesium oxide and strontium oxide as modifiers in silicate-based bioactive glasses: Effects on thermal behaviour, mechanical properties and in-vitro bioactivity. *Materials Science and Engineering: C*, *72*, 566-575.

Bellucci, D., Veronesi, E., Dominici, M., & Cannillo, V. (2020). On the in vitro biocompatibility testing of bioactive glasses. *Materials*, *13*(8), 1816.

Bento, R., Gaddam, A., & Ferreira, J. M. (2021). Sol–gel synthesis and characterization of a quaternary bioglass for bone regeneration and tissue engineering. *Materials*, *14*(16), 4515.

Berridge, M. V., Herst, P. M., & Tan, A. S. (2005). Tetrazolium dyes as tools in cell biology: new insights into their cellular reduction. *Biotechnology annual review*, *11*, 127-152.

Brinker, C. J. (1988). Hydrolysis and condensation of silicates: effects on structure. *Journal of non-crystalline solids*, *100*(1-3), 31-50.

Bromer, F. D., Brent, M. B., Thomsen, J. S., & Brüel, A. (2022). Drill-Hole Bone Defects in Animal Models of Bone Healing: Protocol for a Systematic Review. *JMIR Res Protoc*, *11*(7), e34887. https://doi.org/10.2196/34887

Bueno, O. M. V. M., Herrera, C. L., Bertran, C. A., San-Miguel, M. A., & Lopes, J. H. (2021). An experimental and theoretical approach on stability towards hydrolysis of triethyl phosphate and its effects on the microstructure of sol-gel-derived bioactive silicate glass. *Materials science and engineering: C*, *120*, 111759.

Cannillo, V., Salvatori, R., Bergamini, S., Bellucci, D., & Bertoldi, C. (2022). Bioactive Glasses in Periodontal Regeneration: Existing Strategies and Future Prospects—A Literature Review. *Materials*, *15*(6), 2194.

Cannio, M., Bellucci, D., Roether, J. A., Boccaccini, D. N., & Cannillo, V. (2021). Bioactive glass applications: A literature review of human clinical trials. *Materials*, *14*(18), 5440.

Catauro, M., Bollino, F., Papale, F., & Ciprioti, S. V. (2015). Investigation on bioactivity, biocompatibility, thermal behavior and antibacterial properties of calcium silicate glass coatings containing Ag. *Journal of Non-Crystalline Solids*, *422*, 16-22.

Chakraborty, P. K., Adhikari, J., & Saha, P. (2021). Variation of the properties of sol–gel synthesized bioactive glass 45S5 in organic and inorganic acid catalysts. *Materials Advances*, *2*(1), 413-425.

Chen, F.-M., & Liu, X. (2016). Advancing biomaterials of human origin for tissue engineering. *Progress in polymer science*, *53*, 86-168.

Chen, J., Zeng, L., Chen, X., Liao, T., & Zheng, J. (2018). Preparation and characterization of bioactive glass tablets and evaluation of bioactivity and cytotoxicity in vitro. *Bioactive materials*, *3*(3), 315-321.

Chen, Q. Z., Thompson, I. D., & Boccaccini, A. R. (2006). 45S5 Bioglass®-derived glass–ceramic scaffolds for bone tissue engineering. *Biomaterials*, *27*(11), 2414-2425.

Chen, X., Guo, C., & Zhao, N. (2008). Preparation and characterization of the sol–gel nano-bioactive glasses modified by the coupling agent gamma-aminopropyltriethoxysilane. *Applied surface science*, *255*(2), 466-468.

Chitra, S., Bargavi, P., Durgalakshmi, D., Rajashree, P., & Balakumar, S. (2019). Role of sintering temperature dependent crystallization of bioactive glasses on erythrocyte and cytocompatibility. *Processing and Application of Ceramics*, *13*(1), 12-23. https://doi.org/10.2298/pac1901012c

de Barros Coelho, M., & Magalhães Pereira, M. (2005). Sol–gel synthesis of bioactive glass scaffolds for tissue engineering: effect of surfactant type and concentration. *Journal of Biomedical Materials Research Part B: Applied Biomaterials: An Official Journal of The Society for Biomaterials, The Japanese Society for Biomaterials, and The Australian Society for Biomaterials and the Korean Society for Biomaterials*, *75*(2), 451-456.

De Caluwé, T., Vercruysse, C., Declercq, H., Schaubroeck, D., Verbeeck, R., & Martens, L. (2016). Bioactivity and biocompatibility of two fluoride containing bioactive glasses for dental applications. *Dental Materials*, *32*(11), 1414-1428.

Delloye, C., Banse, X., Brichard, B., Docquier, P.-L., & Cornu, O. (2007). Pelvic Reconstruction with a Structural Pelvic Allograft After Resection of a Malignant Bone Tumor. *JBJS*, *89*(3), 579-587. https://doi.org/10.2106/jbjs.E.00943

Deshmukh, K., Kovářík, T., Křenek, T., Docheva, D., Stich, T., & Pola, J. (2020). Recent advances and future perspectives of sol–gel derived porous bioactive glasses: a review. *RSC advances*, *10*(56), 33782-33835.

Dolan, E. B., Hofmann, B., de Vaal, M. H., Bellavia, G., Straino, S., Kovarova, L., Pravda, M., Velebny, V., Daro, D., & Braun, N. (2019). A bioresorbable biomaterial carrier and passive stabilization device to improve heart function post-myocardial infarction. *Materials Science and Engineering: C*, *103*, 109751.

Drevet, R., Fauré, J., & Benhayoune, H. (2023). Calcium Phosphates and Bioactive Glasses for Bone Implant Applications. In (Vol. 13, pp. 1217): MDPI.

Durgalakshmi, D., Rakkesh, R. A., Aruna, P., Ganesan, S., & Balakumar, S. (2020). Bioactivity and hemocompatibility of sol–gel bioactive glass synthesized under different catalytic conditions. *New Journal of Chemistry*, *44*(48), 21026-21037. https://doi.org/10.1039/d0nj02445g

El-Fiqi, A., Kim, T. H., Kim, M., Eltohamy, M., Won, J. E., Lee, E. J., & Kim, H. W. (2012). Capacity of mesoporous bioactive glass nanoparticles to deliver therapeutic molecules. *Nanoscale*, *4*(23), 7475-7488. https://doi.org/10.1039/c2nr31775c

El-Rashidy, A. A., Roether, J. A., Harhaus, L., Kneser, U., & Boccaccini, A. R. (2017). Regenerating bone with bioactive glass scaffolds: A review of in vivo studies in bone defect models. *Acta biomaterialia*, *62*, 1-28. https://doi.org/https://doi.org/10.1016/j.actbio.2017.08.030

ElBatal, H., Azooz, M., Khalil, E., Monem, A. S., & Hamdy, Y. (2003). Characterization of some bioglass–ceramics. *Materials chemistry and physics*, *80*(3), 599-609.

Faure, J., Drevet, R., Lemelle, A., Jaber, N. B., Tara, A., El Btaouri, H., & Benhayoune, H. (2015). A new sol–gel synthesis of 45S5 bioactive glass using an organic acid as catalyst. *Materials Science and Engineering: C*, *47*, 407-412.

Fernandes, H. R., Gaddam, A., Rebelo, A., Brazete, D., Stan, G. E., & Ferreira, J. M. (2018). Bioactive glasses and glass-ceramics for healthcare applications in bone regeneration and tissue engineering. *Materials*, *11*(12), 2530.

Fernandes, H. R., Gaddam, A., Rebelo, A., Brazete, D., Stan, G. E., & Ferreira, J. M. F. (2018). Bioactive Glasses and Glass-Ceramics for Healthcare Applications in Bone Regeneration and Tissue Engineering. *Materials*, *11*(12), 2530. https://www.mdpi.com/1996-1944/11/12/2530

Fu, Q., Saiz, E., Rahaman, M. N., & Tomsia, A. P. (2011). Bioactive glass scaffolds for bone tissue engineering: state of the art and future perspectives. *Materials Science and Engineering: C*, *31*(7), 1245-1256. https://doi.org/https://doi.org/10.1016/j.msec.2011.04.022

Gao, S., Zhang, H., Lai, L., Xu, M., Yu, H., Qian, A., & Zhang, W. (2024). New technologies for bone diseases. In *Bone Cell Biomechanics, Mechanobiology and Bone Diseases* (pp. 355-376). Elsevier.

Gautam, G., Kumar, S., & Kumar, K. (2022). Processing of biomaterials for bone tissue engineering: State of the art. *Materials today: proceedings*, *50*, 2206-2217.

Ghoneimy, A. M. E., Sherbiny, M. E., & Kamal, N. (2019). Use of Vascularized Fibular Free Flap in the Reconstruction of the Femur in Pediatric and Adolescent Bone Sarcomas: Complications and Functional Outcome. *J Reconstr Microsurg*, *35*(2), 156-162. https://doi.org/10.1055/s-0038-1668142

Graci, C., Maccauro, G., Muratori, F., Spinelli, M. S., Rosa, M. A., & Fabbriciani, C. (2010). Infection following Bone Tumor Resection and Reconstruction with Tumoral Prostheses: A Literature Review. *International Journal of Immunopathology and Pharmacology*, *23*(4), 1005-1013. https://doi.org/10.1177/039463201002300405

Hench, L. L., & Jones, J. R. (2015). Bioactive glasses: frontiers and challenges. *Frontiers in bioengineering and biotechnology*, *3*, 194.

Hench, L. L., & Polak, J. M. (2002). Third-generation biomedical materials. *Science*, *295*(5557), 1014-1017.

Hong, B.-J., Hsiao, C.-W., Bakare, F. F., Sun, J.-T., & Shih, S.-J. (2018). Effect of acetic acid concentration on pore structure for mesoporous bioactive glass during spray pyrolysis. *Materials*, *11*(6), 963.

Hong, B.-J., & Shih, S.-J. (2017). Novel pore-forming agent to prepare of mesoporous bioactive glass using one-step spray pyrolysis. *Ceramics International*, *43*, S771-S775. https://doi.org/10.1016/j.ceramint.2017.05.194

Houreh, A. B., Labbaf, S., Ting, H.-K., Ejeian, F., Jones, J. R., & Esfahani, M.-H. N. (2017). Influence of calcium and phosphorus release from bioactive glasses on viability and differentiation of dental pulp stem cells. *Journal of Materials Science*, *52*, 8928-8941.

Hsu, F.-Y., Hsu, H.-W., Chang, Y.-H., Yu, J.-L., Rau, L.-R., & Tsai, S.-W. (2018). Macroporous microbeads containing apatite-modified mesoporous bioactive glass nanofibres for bone tissue engineering applications. *Materials Science and Engineering: C*, *89*, 346-354.

Hu, M., Fang, J., Zhang, Y., Wang, X., Zhong, W., & Zhou, Z. (2020). Design and evaluation a kind of functional biomaterial for bone tissue engineering: Selenium/mesoporous bioactive glass nanospheres. *Journal of Colloid and Interface Science*, *579*, 654-666.

Ingole, V., Sathe, B., & Ghule, A. (2018). Bioactive ceramic composite material stability, characterization. *Fundamental biomaterials: ceramics*, 273-296.

Islam, M. T., Felfel, R. M., Abou Neel, E. A., Grant, D. M., Ahmed, I., & Hossain, K. M. Z. (2017). Bioactive calcium phosphate–based glasses and ceramics and their biomedical applications: a review. *Journal of tissue engineering*, *8*, 2041731417719170.

Izquierdo-Barba, I., Martinez, Á., Doadrio, A. L., Pérez-Pariente, J., & Vallet-Regí, M. (2005). Release evaluation of drugs from ordered three-dimensional silica structures. *European Journal of Pharmaceutical Sciences*, *26*(5), 365-373.

Jafari, N., Habashi, M. S., Hashemi, A., Shirazi, R., Tanideh, N., & Tamadon, A. (2022). Application of bioactive glasses in various dental fields. *Biomaterials Research*, *26*(1), 31.

Jang, J.-H., Lee, M. G., Ferracane, J. L., Davis, H., Bae, H. E., Choi, D., & Kim, D.-S. (2018). Effect of bioactive glass-containing resin composite on dentin remineralization. *Journal of dentistry*, *75*, 58-64.

Jones, J. R., Ehrenfried, L. M., & Hench, L. L. (2006). Optimising bioactive glass scaffolds for bone tissue engineering. *Biomaterials*, *27*(7), 964-973.

Joy-anne, N. O., Su, Y., Lu, X., Kuo, P.-H., Du, J., & Zhu, D. (2019). Bioactive glass coatings on metallic implants for biomedical applications. *Bioactive materials*, *4*, 261-270.

Kaou, M. H., Furkó, M., Balázsi, K., & Balázsi, C. (2023). Advanced Bioactive Glasses: The Newest Achievements and Breakthroughs in the Area. *Nanomaterials*, *13*(16), 2287.

Kapoor, S., Goel, A., Tilocca, A., Dhuna, V., Bhatia, G., Dhuna, K., & Ferreira, J. M. (2014). Role of glass structure in defining the chemical dissolution behavior, bioactivity and antioxidant properties of zinc and strontium co-doped alkali-free phosphosilicate glasses. *Acta Biomaterialia*, *10*(7), 3264-3278.

Kargozar, S., Montazerian, M., Hamzehlou, S., Kim, H.-W., & Baino, F. (2018). Mesoporous bioactive glasses: Promising platforms for antibacterial strategies. *Acta Biomaterialia*, *81*, 1-19.

Kaur, G., Pandey, O. P., Singh, K., Homa, D., Scott, B., & Pickrell, G. (2014). A review of bioactive glasses: their structure, properties, fabrication and apatite formation. *Journal of Biomedical Materials Research Part A: An Official Journal of The Society for Biomaterials, The Japanese Society for Biomaterials, and The Australian Society for Biomaterials and the Korean Society for Biomaterials*, *102*(1), 254-274.

Kaur, P., Singh, K., Kaur, S., Kaur, S., & Singh, A. P. (2020). Sol-gel derived strontium-doped SiO2–CaO–MgO–P2O5 bioceramics for faster growth of bone like hydroxyapatite and their in vitro study for orthopedic applications. *Materials Chemistry and Physics*, *245*, 122763.

Khalid, M. D., Khurshid, Z., Zafar, M. S., Farooq, I., Khan, R. S., & Najmi, A. (2017). Bioactive Glasses and their Applications in Dentistry. *Journal of The Pakistan Dental Association*, *26*(1).

Kim, T., See, C. W., Li, X., & Zhu, D. (2020). Orthopedic implants and devices for bone fractures and defects: Past, present and perspective. *Engineered Regeneration*, *1*, 6-18. https://doi.org/https://doi.org/10.1016/j.engreg.2020.05.003

Kokubo, T., & Yamaguchi, S. (2019). Simulated body fluid and the novel bioactive materials derived from it. *Journal of Biomedical Materials Research Part A*, *107*(5), 968-977.

Kuo, C.-K., Chen, L.-G., Tseng, C.-F., & Chou, Y.-J. (2021). Influences of acid catalysts on the microstructure, bioactivity and cytotoxicity of bioactive glass nanoparticles prepared by spray pyrolysis. *Journal of Non-Crystalline Solids*, *560*, 120710.

Lee, W., Debasitis, J. C., Lee, V. K., Lee, J.-H., Fischer, K., Edminster, K., Park, J.-K., & Yoo, S.-S. (2009). Multi-layered culture of human skin fibroblasts and keratinocytes through three-dimensional freeform fabrication. *Biomaterials*, *30*(8), 1587-1595.

Lei, B., Chen, X., & Koh, Y.-H. (2011). Effects of acidic catalysts on the microstructure and biological property of sol–gel bioactive glass microspheres. *Journal of sol-gel science and technology*, *58*, 656-663.

Lei, B., Chen, X., Wang, Y., & Zhao, N. (2009). Synthesis and in vitro bioactivity of novel mesoporous hollow bioactive glass microspheres. *Materials Letters*, *63*(20), 1719-1721.

Lei, B., Chen, X., Wang, Y., Zhao, N., Du, C., & Zhang, L. (2009). Acetic acid derived mesoporous bioactive glasses with an enhanced in vitro bioactivity. *Journal of non-crystalline solids*, *355*(52-54), 2583-2587.

Lei, Q., Guo, J., Noureddine, A., Wang, A., Wuttke, S., Brinker, C. J., & Zhu, W. (2020). Sol–gel-based advanced porous silica materials for biomedical applications. *Advanced Functional Materials*, *30*(41), 1909539.

Leite, Á. J., & Mano, J. (2017). Biomedical applications of natural-based polymers combined with bioactive glass nanoparticles. *Journal of materials chemistry B*, *5*(24), 4555-4568.

Lemyre, J.-L., & Ritcey, A. M. (2010). Characterization of a reverse micellar system by 1H NMR. *Langmuir*, *26*(9), 6250-6255.

Letaïef, N., Lucas-Girot, A., Oudadesse, H., Dorbez-Sridi, R., & Boullay, P. (2014). Investigation of the surfactant type effect on characteristics and bioactivity of new mesoporous bioactive glass in the ternary system SiO2–CaO–P2O5: Structural, textural and reactivity studies. *Microporous and mesoporous materials*, *195*, 102-111.

Letaief, N., Lucas-Girot, A., Oudadesse, H., Meleard, P., Pott, T., Jelassi, J., & Dorbez-Sridi, R. (2014). Effect of aging temperature on the structure, pore morphology and bioactivity of new sol–gel synthesized bioglass. *Journal of non-crystalline solids*, *402*, 194-199.

Li, H., & Chang, J. (2013). Bioactive silicate materials stimulate angiogenesis in fibroblast and endothelial cell co-culture system through paracrine effect. *Acta biomaterialia*, *9*(6), 6981-6991.

Li, N., Jie, Q., Zhu, S., & Wang, R. (2004). A new route to prepare macroporous bioactive sol–gel glasses with high mechanical strength. *Materials Letters*, *58*(22-23), 2747-2750.

Li, Y., Chen, X., Ning, C., Yuan, B., & Hu, Q. (2015). Facile synthesis of mesoporous bioactive glasses with controlled shapes. *Materials Letters*, *161*, 605-608.

Lopes, J. H., Bueno, O. M. V. M., Mazali, I. O., & Bertran, C. A. (2019). Investigation of citric acid-assisted sol-gel synthesis coupled to the self-propagating combustion method for preparing bioactive glass with high structural homogeneity. *Materials Science and Engineering: C*, *97*, 669-678.

Lu, Y., Wang, J., Yang, Y., & Yin, Q. (2021). Bone defects are repaired by enhanced osteogenic activity of the induced membrane: a case report and literature review. *BMC Musculoskeletal Disorders*, *22*(1), 447. https://doi.org/10.1186/s12891-021-04317-2

Lutzweiler, G., Ndreu Halili, A., & Engin Vrana, N. (2020). The overview of porous, bioactive scaffolds as instructive biomaterials for tissue regeneration and their clinical translation. *Pharmaceutics*, *12*(7), 602.

Mahdi, O. S. (2019). Bioactive glasses in dental applications (literature review). *Journal of University of Babylon for Engineering Sciences*, *27*(2), 207-213.

Mankin, H. J., Hornicek, F. J., & Raskin, K. A. (2005). Infection in Massive Bone Allografts. *Clinical Orthopaedics and Related Research (1976-2007)*, *432*, 210-216. https://doi.org/10.1097/01.blo.0000150371.77314.52

Mayfield, C. K., Ayad, M., Lechtholz-Zey, E., Chen, Y., & Lieberman, J. R. (2022). 3D-Printing for Critical Sized Bone Defects: Current Concepts and Future Directions. *Bioengineering*, *9*(11), 680. https://www.mdpi.com/2306-5354/9/11/680

Mazzoni, E., Iaquinta, M. R., Lanzillotti, C., Mazziotta, C., Maritati, M., Montesi, M., Sprio, S., Tampieri, A., Tognon, M., & Martini, F. (2021). Bioactive materials for soft tissue repair. *Frontiers in bioengineering and biotechnology*, *9*, 613787.

Miao, G., Chen, X., Dong, H., Fang, L., Mao, C., Li, Y., Li, Z., & Hu, Q. (2013). Investigation of emulsified, acid and acid-alkali catalyzed mesoporous bioactive glass microspheres for bone regeneration and drug delivery. *Materials Science and Engineering: C*, *33*(7), 4236-4243.

Miao, X., & Sun, D. (2009). Graded/gradient porous biomaterials. *Materials*, *3*(1), 26-47.

Migliorini, F., La Padula, G., Torsiello, E., Spiezia, F., Oliva, F., & Maffulli, N. (2021). Strategies for large bone defect reconstruction after trauma, infections or tumour excision: a comprehensive review of the literature. *Eur J Med Res*, *26*(1), 118. https://doi.org/10.1186/s40001-021-00593-9

Migneco, C., Fiume, E., Verné, E., & Baino, F. (2020). A guided walk through the world of mesoporous bioactive glasses (MBGs): Fundamentals, processing, and applications. *Nanomaterials*, *10*(12), 2571.

Min, Z., Huixue, W., Yujie, Z., Lixin, J., Hai, H., & Yufang, Z. (2016). Synthesis of monodispersed mesoporous bioactive glass nanospheres for bone repair. *Materials Letters*, *171*, 259-262.

Moghanian, A., Firoozi, S., & Tahriri, M. (2017). Characterization, in vitro bioactivity and biological studies of sol-gel synthesized SrO substituted 58S bioactive glass. *Ceramics International*, *43*(17), 14880-14890.

Moghanian, A., Koohfar, A., Hosseini, S., Hosseini, S. H., Ghorbanoghli, A., Sajjadnejad, M., Raz, M., Elsa, M., & Sharifianjazi, F. (2021). Synthesis, characterization and in vitro biological properties of simultaneous co-substituted Ti+ 4/Li+ 1 58s bioactive glass. *Journal of Non-Crystalline Solids*, *561*, 120740.

Montazerian, M., & Zanotto, E. D. (2017). A guided walk through Larry Hench's monumental discoveries. *Journal of Materials Science*, *52*(15), 8695-8732.

Moritz, M., & Geszke-Moritz, M. (2022). Mesoporous materials as elements of modern drug delivery systems for anti-inflammatory agents: A review of recent achievements. *Pharmaceutics*, *14*(8), 1542.

Motta, C., Cavagnetto, D., Amoroso, F., Baldi, I., & Mussano, F. (2023). Bioactive glass for periodontal regeneration: a systematic review. *BMC Oral Health*, *23*(1), 264. https://doi.org/10.1186/s12903-023-02898-z

Mukundan, L. M., Nirmal, R., Vaikkath, D., & Nair, P. D. (2013). A new synthesis route to high surface area sol gel bioactive glass through alcohol washing: a preliminary study. *Biomatter*, *3*(2). https://doi.org/10.4161/biom.24288

Naruphontjirakul, P., Li, S., Pinna, A., Barrak, F., Chen, S., Redpath, A. N., Rankin, S. M., Porter, A. E., & Jones, J. R. (2022). Interaction of monodispersed strontium containing bioactive glass nanoparticles with macrophages. *Biomaterials Advances*, *133*, 112610.

Nejati Rad, H., Behnamghader, A., Bagheri, M., & Mozafari, M. (2020). Effect of Surfactant type on the Characteristics and Bioactivity of Mesoporous Bioactive Glasses. *Advanced Materials Letters*, *11*(8), 1-7.

Nishida, J., & Shimamura, T. (2008). Methods of reconstruction for bone defect after tumor excision: a review of alternatives. *Medical science monitor : international medical journal of experimental and clinical research*, *14*(8), RA107-113. http://europepmc.org/abstract/MED/18668007

Nkenke, E., & Neukam, F. W. (2014). Autogenous bone harvesting and grafting in advanced jaw resorption: morbidity, resorption and implant survival. *Eur J Oral Implantol*, *7*(Suppl 2), S203-S217.

Ou, Q., Wu, P., Zhou, Z., Pan, D., & Tang, J.-y. (2020). Complication of osteo reconstruction by utilizing free vascularized fibular bone graft. *BMC Surgery*, *20*(1), 216. https://doi.org/10.1186/s12893-020-00875-9

ÖZEL, C., KIZIL, P., EMİR, C., & YÜCEL, S. THE USAGE OF BIOACTIVE GLASSES IN BONE TISSUE ENGINEERING.

Panagopoulos, G. N., Mavrogenis, A. F., Mauffrey, C., Lesensky, J., Angelini, A., Megaloikonomos, P. D., Igoumenou, V. G., Papanastassiou, J., Savvidou, O., Ruggieri, P., & Papagelopoulos, P. J. (2017). Intercalary reconstructions after bone tumor resections: a review of treatments. *Eur J Orthop Surg Traumatol*, *27*(6), 737-746. https://doi.org/10.1007/s00590-017-1985-x

Panagopoulos, G. N., Mavrogenis, A. F., Mauffrey, C., Lesenský, J., Angelini, A., Megaloikonomos, P. D., Igoumenou, V. G., Papanastassiou, J., Savvidou, O., Ruggieri, P., & Papagelopoulos, P. J. (2017). Intercalary reconstructions after bone tumor resections: a review of treatments. *European Journal of Orthopaedic Surgery & Traumatology*, *27*(6), 737-746. https://doi.org/10.1007/s00590-017-1985-x

Peng, T.-Y., Tsai, P.-Y., Chen, M.-S., Mine, Y., Wu, S.-H., Chen, C.-Y., Lin, D.-J., & Lin, C.-K. (2021). Mesoporous properties of bioactive glass synthesized by spray pyrolysis with various polyethylene glycol and acid additions. *Polymers*, *13*(4), 618.

Rahaman, M. N., Day, D. E., Bal, B. S., Fu, Q., Jung, S. B., Bonewald, L. F., & Tomsia, A. P. (2011). Bioactive glass in tissue engineering. *Acta biomaterialia*, *7*(6), 2355-2373.

Ratner, B. D., & Zhang, G. (2020). A history of biomaterials. In *Biomaterials Science* (pp. 21-34). Elsevier.

Ravarian, R., Moztarzadeh, F., Hashjin, M. S., Rabiee, S., Khoshakhlagh, P., & Tahriri, M. (2010). Synthesis, characterization and bioactivity investigation of bioglass/hydroxyapatite composite. *Ceramics International*, *36*(1), 291-297.

Renard, A. J., Veth, R. P., Schreuder, H. W. B., van Loon, C. J., Koops, H. S., & van Horn, J. R. (2000). Function and complications after ablative and limb-salvage therapy in lower extremity sarcoma of bone. *Journal of Surgical Oncology*, *73*(4), 198-205. https://doi.org/https://doi.org/10.1002/(SICI)1096-9098(200004)73:4<198::AID-JSO3>3.0.CO;2-X

Rezaei, Y., Moztarzadeh, F., Shahabi, S., & Tahriri, M. (2014). Synthesis, characterization, and in vitro bioactivity of sol-gel-derived SiO2–CaO–P2O5–MgO-SrO bioactive glass. *Synthesis and Reactivity in Inorganic, Metal-Organic, and Nano-Metal Chemistry*, *44*(5), 692-701.

Salinas, A., Vallet-Regi, M., & Heikkilä, J. (2018). Use of bioactive glasses as bone substitutes in orthopedics and traumatology. In *Bioactive glasses* (pp. 337-364). Elsevier.

Salonen, J., Laitinen, L., Kaukonen, A. M., Tuura, J., Björkqvist, M., Heikkilä, T., Vähä-Heikkilä, K., Hirvonen, J., & Lehto, V.-P. (2005). Mesoporous silicon microparticles for oral drug delivery: loading and release of five model drugs. *Journal of controlled release*, *108*(2-3), 362-374.

Santos, S. C., Barreto, L. S., & dos Santos, E. A. (2016). Nanocrystalline apatite formation on bioactive glass in a sol–gel synthesis. *Journal of Non-Crystalline Solids*, *439*, 30-37.

Sanz-Herrera, J., & Boccaccini, A. (2011). Modelling bioactivity and degradation of bioactive glass based tissue engineering scaffolds. *International Journal of Solids and Structures*, *48*(2), 257-268.

Saravanapavan, P., Jones, J. R., Verrier, S., Beilby, R., Shirtliff, V. J., Hench, L. L., & Polak, J. M. (2004). Binary CaO–SiO 2 gel-glasses for biomedical applications. *Bio-Medical Materials and Engineering*, *14*(4), 467-486.

Sathiskumar, S., Vanaraj, S., Sabarinathan, D., Bharath, S., Sivarasan, G., Arulmani, S., Preethi, K., & Ponnusamy, V. K. (2019). Green synthesis of biocompatible nanostructured hydroxyapatite from Cirrhinus mrigala fish scale–A biowaste to biomaterial. *Ceramics International*, *45*(6), 7804-7810.

Schmitz, S., Beltrán, A. M., Cresswell, M., & Boccaccini, A. R. (2020). A Structural comparison of ordered and non-ordered ion doped silicate bioactive glasses. *Materials*, *13*(4), 992.

Schumacher, M., Habibovic, P., & Van Rijt, S. (2021). Mesoporous bioactive glass composition effects on degradation and bioactivity. *Bioactive Materials*, *6*(7), 1921-1931.

Sepulveda, P., Jones, J. R., & Hench, L. L. (2002). Bioactive sol-gel foams for tissue repair. *Journal of Biomedical Materials Research: An Official Journal of The Society for Biomaterials, The Japanese Society for Biomaterials, and The Australian Society for Biomaterials and the Korean Society for Biomaterials*, *59*(2), 340-348.

Serra, J., González, P., Liste, S., Serra, C., Chiussi, S., León, B., Pérez-Amor, M., Ylänen, H., & Hupa, M. (2003). FTIR and XPS studies of bioactive silica based glasses. *Journal of Non-Crystalline Solids*, *332*(1-3), 20-27.

Shearer, A., Molinaro, M., Montazerian, M., Sly, J. J., Miola, M., Baino, F., & Mauro, J. C. (2024). The unexplored role of alkali and alkaline earth elements (ALAEs) on the structure, processing, and biological effects of bioactive glasses. *Biomaterials Science*.

Shearer, A., Montazerian, M., & Mauro, J. C. (2023). Modern definition of bioactive glasses and glass-ceramics. *Journal of Non-Crystalline Solids*, *608*, 122228.

Shibuya, N., & Jupiter, D. C. (2015). Bone graft substitute: allograft and xenograft. *Clinics in podiatric medicine and surgery*, *32*(1), 21-34.

Shih, S.-J., Chou, Y.-J., & Chien, I.-C. (2012). One-step synthesis of bioactive glass by spray pyrolysis. *Journal of Nanoparticle Research*, *14*, 1-8.

Shih, S.-J., Lin, Y.-C., Valentino Posma Panjaitan, L., & Rahayu Meyla Sari, D. (2016). The correlation of surfactant concentrations on the properties of mesoporous bioactive glass. *Materials*, *9*(1), 58.

Shih, S. J., Sari, D. R. M., & Lin, Y. C. (2016). Influence of Chemical Composition on the Bioactivity of Spray Pyrolyzed Mesoporous Bioactive Glass. *International Journal of Applied Ceramic Technology*, *13*(4), 787-794. https://doi.org/10.1111/ijac.12552

Sierra, L., Lopez, B., & Guth, J.-L. (2000). Preparation of mesoporous silica particles with controlled morphology from sodium silicate solutions and a non-ionic surfactant at pH values between 2 and 6. *Microporous and mesoporous materials*, *39*(3), 519-527.

Siqueira, R. L., Maurmann, N., Burguêz, D., Pereira, D. P., Rastelli, A. N., Peitl, O., Pranke, P., & Zanotto, E. D. (2017). Bioactive gel-glasses with distinctly different compositions: bioactivity, viability of stem cells and antibiofilm effect against Streptococcus mutans. *Materials Science and Engineering: C*, *76*, 233-241.

Solgi, S., Khakbiz, M., Shahrezaee, M., Zamanian, A., Tahriri, M., Keshtkari, S., Raz, M., Khoshroo, K., Moghadas, S., & Rajabnejad, A. (2017). Synthesis, characterization and in vitro biological evaluation of sol-gel derived Sr-containing nano bioactive glass. *Silicon*, *9*(4), 535-542.

Subramani, K., & Ahmed, W. (2012). *Nanobiomaterials in clinical dentistry*. William Andrew.

Tainio, J., Paakinaho, K., Ahola, N., Hannula, M., Hyttinen, J., Kellomäki, M., & Massera, J. (2017). In vitro degradation of borosilicate bioactive glass and poly (l-lactide-co-ε-caprolactone) composite scaffolds. *Materials*, *10*(11), 1274.

Thavornyutikarn, B., Feltis, B., Wright, P. F., & Turney, T. W. (2019). Effect of pre-treatment of crystallized bioactive glass with cell culture media on structure, degradability, and biocompatibility. *Materials Science and Engineering: C*, *97*, 188-197.

Thommes, M., Kaneko, K., Neimark, A. V., Olivier, J. P., Rodriguez-Reinoso, F., Rouquerol, J., & Sing, K. S. (2015). Physisorption of gases, with special reference to the evaluation of surface area and pore size distribution (IUPAC Technical Report). *Pure and applied chemistry*, *87*(9-10), 1051-1069.

Vafa, E., Bazargan-Lari, R., & Bahrololoom, M. E. (2021). Synthesis of 45S5 bioactive glass-ceramic using the sol-gel method, catalyzed by low concentration acetic acid extracted from homemade vinegar. *Journal of Materials Research and Technology*, *10*, 1427-1436. https://doi.org/10.1016/j.jmrt.2020.12.093

Vallet-Regí, M., Izquierdo-Barba, I., Rámila, A., Pérez-Pariente, J., Babonneau, F., & González-Calbet, J. M. (2005). Phosphorous-doped MCM-41 as bioactive material. *Solid state sciences*, *7*(2), 233-237.

Vallet-Regí, M. (2010). Nanostructured mesoporous silica matrices in nanomedicine. *Journal of internal medicine*, *267*(1), 22-43.

Vallet-Regí, M., Izquierdo-Barba, I., & Salinas, A. (1999). Influence of P2O5 on crystallinity of apatite formed in vitro on surface of bioactive glasses. *Journal of Biomedical Materials Research: An Official Journal of The Society for Biomaterials, The Japanese Society for Biomaterials, and The Australian Society for Biomaterials and the Korean Society for Biomaterials*, *46*(4), 560-565.

Vichery, C., & Nedelec, J.-M. (2016). Bioactive glass nanoparticles: From synthesis to materials design for biomedical applications. *Materials*, *9*(4), 288.

Workie, A. B., Ningsih, H. S., & Shih, S.-J. (2023). An comprehensive review on the spray pyrolysis technique: historical context, operational factors, classifications, and product applications. *Journal of Analytical and Applied Pyrolysis*, 105915.

Wu, C., & Chang, J. (2011). Mesoporous bioactive glasses: structure characteristics, drug/growth factor delivery and bone regeneration application. Interface Focus 2: 292–306. *Robocasting of mesoporous bioactive glasses (MBGs)*, *347*.

Wu, C., & Chang, J. (2012). Mesoporous bioactive glasses: Structure characteristics, drug/growth factor delivery and bone regeneration application. *Interface focus*, *2*(3), 292-306.

Xia, W., & Chang, J. (2006). Well-ordered mesoporous bioactive glasses (MBG): a promising bioactive drug delivery system. *Journal of Controlled Release*, *110*(3), 522-530.

Xia, W., & Chang, J. (2007). Preparation and characterization of nano-bioactive-glasses (NBG) by a quick alkali-mediated sol–gel method. *Materials letters*, *61*(14-15), 3251-3253.

Xue, N., Ding, X., Huang, R., Jiang, R., Huang, H., Pan, X., Min, W., Chen, J., Duan, J.-A., Liu, P., & Wang, Y. (2022). Bone Tissue Engineering in the Treatment of Bone Defects. *Pharmaceuticals*, *15*(7), 879. https://www.mdpi.com/1424-8247/15/7/879

Xynos, I. D., Edgar, A. J., Buttery, L. D., Hench, L. L., & Polak, J. M. (2001). Gene-expression profiling of human osteoblasts following treatment with the ionic products of Bioglass® 45S5 dissolution. *Journal of Biomedical Materials Research: An Official Journal of The Society for Biomaterials, The Japanese Society for Biomaterials, and The Australian Society for Biomaterials and the Korean Society for Biomaterials*, *55*(2), 151-157.

Yan, X., Huang, X., Yu, C., Deng, H., Wang, Y., Zhang, Z., Qiao, S., Lu, G., & Zhao, D. (2006). The in-vitro bioactivity of mesoporous bioactive glasses. *Biomaterials*, *27*(18), 3396-3403.

Yan, X., Yu, C., Zhou, X., Tang, J., & Zhao, D. (2004). Highly ordered mesoporous bioactive glasses with superior in vitro bone-forming bioactivities. *Angewandte Chemie International Edition*, *43*(44), 5980-5984.

Zekry, K. M., Yamamoto, N., Hayashi, K., Takeuchi, A., Alkhooly, A. Z. A., Abd-Elfattah, A. S., Elsaid, A. N. S., Ahmed, A. R., & Tsuchiya, H. (2019). Reconstruction of intercalary bone defect after resection of malignant bone tumor. *J Orthop Surg (Hong Kong)*, *27*(1), 2309499019832970. https://doi.org/10.1177/2309499019832970

Zhang, J., Jiang, Y., Shang, Z., Zhao, B., Jiao, M., Liu, W., Cheng, M., Zhai, B., Guo, Y., Liu, B., Shi, X., & Ma, B. (2021). Biodegradable metals for bone defect repair: A systematic review and meta-analysis based on animal studies. *Bioactive Materials*, *6*(11), 4027-4052. https://doi.org/https://doi.org/10.1016/j.bioactmat.2021.03.035

Zhao, Y., Zhang, Z., Pan, Z., & Liu, Y. (2021). Advanced bioactive nanomaterials for biomedical applications. Exploration,

Zheng, K., & Boccaccini, A. R. (2017). Sol-gel processing of bioactive glass nanoparticles: A review. *Advances in Colloid and Interface Science*, *249*, 363-373.

Zheng, K., Niu, W., Lei, B., & Boccaccini, A. R. (2021). Immunomodulatory bioactive glasses for tissue regeneration. *Acta Biomaterialia*, *133*, 168-186.

Zheng, K., Sui, B., Ilyas, K., & Boccaccini, A. R. (2021). Porous bioactive glass micro-and nanospheres with controlled morphology: Developments, properties and emerging biomedical applications. *Materials Horizons*, *8*(2), 300-335.

Zheng, K., Torre, E., Bari, A., Taccardi, N., Cassinelli, C., Morra, M., Fiorilli, S., Vitale-Brovarone, C., Iviglia, G., & Boccaccini, A. R. (2020). Antioxidant mesoporous Ce-doped bioactive glass nanoparticles with anti-inflammatory and pro-osteogenic activities. *Materials Today Bio*, *5*, 100041.

Zheng, K., Yu, X. C., Hu, Y. C., Shao, Z. W., Xu, M., Wang, B. C., & Wang, F. (2019). Outcome of segmental prosthesis reconstruction for diaphyseal bone tumors: a multi-center retrospective study. *BMC Cancer*, *19*(1), 638. https://doi.org/10.1186/s12885-019-5865-0

Zhu, Y., Wu, C., Ramaswamy, Y., Kockrick, E., Simon, P., Kaskel, S., & Zreiqat, H. (2008). Preparation, characterization and in vitro bioactivity of mesoporous bioactive glasses (MBGs) scaffolds for bone tissue engineering. *Microporous and Mesoporous Materials*, *112*(1-3), 494-503.